D6.1.2: Survey report on interference sources in smart grid

Revision History

Edition	Date	Status	Editor
v0.1	13.12.2011	first draft	S. Horsmanheimo H. Kokkoniemi-Tarkkanen P. Savolainen L. Tuomimäki
v.0.2	18.12.2011	updates	P. Muszynski L. Helenius S. Horsmanheimo
v.0.3	19.12.2011	updates	J. Penttonen S. Horsmanheimo
v.0.4	21.12.2011	updates	S. Horsmanheimo H. Kokkoniemi-Tarkkanen P. Savolainen
v.1.0	29.12.2011	submitted	S. Horsmanheimo J. Penttonen

Abstract

The motivation of this report was to study the feasibility of existing commercial 2G (GSM900) and 3G (UMTS900) networks for Smart Grids to support remote control and metering in rural and suburban areas. These wireless networks are found compelling because they are mass market products providing wide-area voice and broadband data services to whole Finland. Furthermore, over several decades their performance and robustness have been validated by a vast number of end-users. At the same time, device and data transmission costs have significantly dropped making them competitive against dedicated wireless control systems.

The research challenge is to proof that these 2G/3G and later 4G networks are sufficient to provide required coverage, redundancy and capacity for Smart Grid communication also in sparsely populated areas, to assess how vulnerable these commercial communication networks are to small or large electric distribution network break downs e.g. caused by heavy storms, and to find a concrete strategy to make wireless communication networks for Smart Grids orders of magnitude more resilient and reliable without additional costs.

The approach that we have taken in our work is to simulate the performance of 2G and 3G networks in different failure scenarios. Raasepori region was selected for the study area, because it contains both suburban and rural regions. Both 2G and 3G networks are available, and it is convenient for both VTT and Viola Systems to arrange field measurements in order to fine-tune and validate calculation models. For the area, an accurate 3D environment model was constructed including terrain height and clutter information. Configurations for communication and electric distribution networks were made using information obtained from other SGEM partners and literature surveys. Preliminary simulations have been carried out using a network planning tool that VTT has been developing over the years. This tool has been tailored and new algorithms have been added to enable the 2G/3G feasibility assessment from the Smart Grid's viewpoint.

This report presents the progress of VTT's and Viola Systems' work in Task 6.1 over a six-month period. This work has also included expert assistance from NSN, TeliaSonera and ABB. The report describes simulation scenarios that have been designed after several technical meetings. The report shows the steps required for creating a 3D environment model. It gives an overview of the RF parameters that are needed for modeling 2G/3G networks. One chapter is devoted to the modeling of an electric distribution network. This was made possible by the input from ABB and Fortum. The rest of the report describes the preliminary simulations results and field measurements performed in fall. The field measurements were used for the propagation model calibration and validation. The last chapter sums up the work done so far and the plans for the FP3. The aim of this report is to create a solid base for more in-depth simulations and analyses that will be carried out in year 2012 in order to study under which conditions the existing GSM900 and UMTS900 communication networks can satisfy the communication requirements of the future Smart Grid systems.

Table of Contents

1 Preface

This report was done as a part of the Finnish national research project "Smart Grid and Energy Market" SGEM Phase 2 and it was funded by Tekes – the Finnish Funding Agency for Technology and Innovation and the project partners. The report was written by VTT, Viola Systems (Jyrki Penttonen and Lauri Helenius) and NSN (Peter Muszynski)

For the report, valuable contributions and comments were obtained from TeliaSonera (Mikko Keto) and ABB (Antti Kostiainen and Dick Kronman).

2 Background

The objective of the work was to carry out a literature survey where different types of interference sources (e.g. external systems that deliberately jam, intra-system and inter-system interference) in Smart Grids are studied. The study was planned to cover both signal propagation and interference mechanisms in 3G/4G communication. The focus of the study was changed to the redundancy analysis, because the reliability and availability of communication systems was found to be more important for electric distribution companies than pure interference analysis. The overlapping cells have positive effects on the Smart Grids by providing better availability in all operational situations.

Smart Grid is fundamentally about creating additional intelligence to the electrical distribution network. Faults must be detected, isolated and resolved quickly and efficiently. As a result, traditional electric distribution networks are undergoing fundamental changes due to Smart Grid initiatives and the increasing pressure by the regulators to improve the quality of energy distribution to households and industry e.g. [1].

- Remote metering at consumer premises has become de facto standard for all electrical utilities.
- More efficient operations to detect faults, to repair them and restore power supply in problem situations are increasingly demanded by regulators and electrical customers.
- Proliferating introduction of solar and wind power means, that the distribution grid needs to be controlled in real-time.
- Making distribution grid smart means, that consumers have full visibility of their electricity usage as they see their billing real-time. This makes it possible to facilitate significant energy savings.
- Smarter grid will make it possible for electrical utility to turn on and off electrical loads so as to cut down peak consumption, thus saving in infrastructure and energy costs.

For all these needs it is important, that a reliable and always-on communication link exists to all of the assets in the distribution network. Traditionally, electric distribution companies have used private communication networks to control their assets such as substations, reclosers, disconnectors and transformers. Proprietary technologies such as microwave links, narrow band VHF/UHF radios, and private mobile radios were often applied. Today, GPRS, EDGE and 3G cellular packet based networks make always-on data connection available to any asset anywhere with much lower costs. Those networks are proof-tested in mass markets, and their availability and reliability will improve even more when the public wireless systems’ convergence is realized. Recently, GPRS, EDGE and 3G networks have recently been used in distribution automation projects. For example, Vattenfall has automated its reclosers and disconnectors using GPRS to connect these entities to the Scada [2]. Electricity Supply Board (ESB) in Ireland has implemented a nation-wide system, where all disconnectors and reclosers have always-on connection to Scada [3].

Although fundamental changes are anticipated, the future intelligent utility networks can extensively utilize existing infrastructures. Moreover, new overlay technologies will gradually be added to the Smart Grids to provide required smart a.k.a cognitive functionalities. As a result, the existing physical power transmission and distribution networks will not need to be extensively modified.

Smart Grid system can be modeled with 3-layer architecture [4] shown in Figure 1:

- **Application layer:** includes applications and services that are available in the Smart Grid. These applications are already being developed or at least envisioned.
- **Communications layer:** includes different types of fixed or wireless communication solutions for end-to-end two-way communication. It glues the physical and application layers together enabling Smart Grid functionalities. Different communication systems will be converged in the future providing better overall availability.
- **Physical power layer:** includes the physical power components of the electric distribution network between a power station and an end-user.

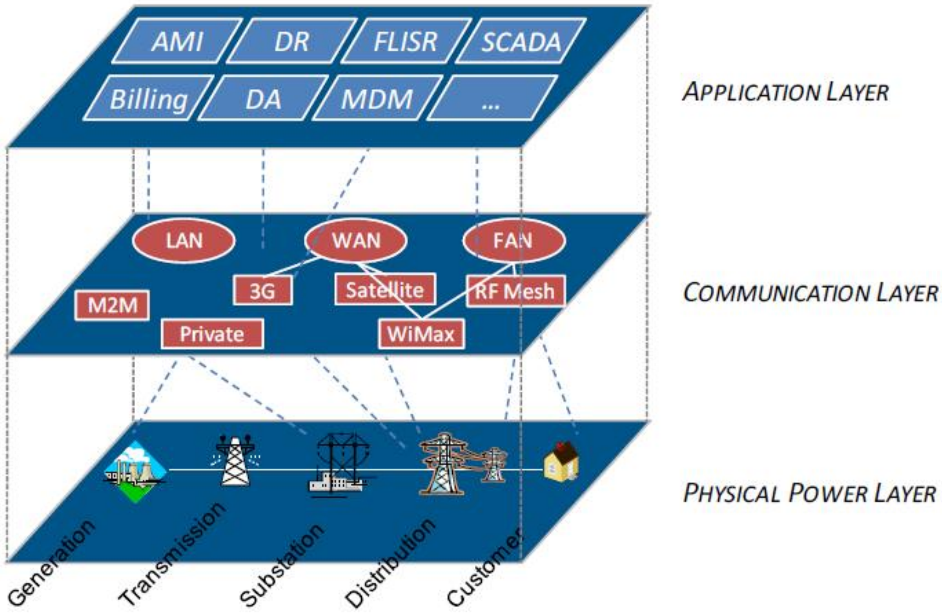

Figure 1. The 3-layer Smart Grid architecture [4].

In this study we are focusing on the reliability and redundancy aspects of using public wireless communications, such as GPRS, EDGE, 3G and LTE, when applying them to electrical distribution network automation. Electrical networks are the core infrastructure of any society. Therefore, requirements for communications reliability are high.

However, until now, no research has been made to provide an analytical framework to assess reliability and redundancy aspects of GPRS/EDGE and 3G for distribution automation applications. The motivation of our study is to provide this framework. The framework is used to model the radio performance of GPRS and 3G networks, when they are applied to control and monitor assets in electrical distribution networks. The radio propagation model is specifically developed so, that it takes into consideration the improved radio performance in typical communication nodes used in distribution automation. The scope of this work covers feeder automation. Background information on feeder automation can be found from SGEM FP1 deliverable [14] and references [17,18]. Network elements of commercial wireless communication networks typically have regulatory requirements for minimum battery backup durations times and also for the possibility for alternative power feed. In the case of Finland, these requirements were presented in SGEM FP1 deliverable [14]. Due to the relevance for the present study a brief synopsis of the power back-up requirements for base stations is extracted from [14] into Appendix 1.

3 Scenarios

For this study, the following requirements were identified as the basis for the scenarios [4]:

- Communications should operate in crisis situations, for example when a storm has cut off electricity from large areas.
- Communication should be always on, so that control centre can monitor the status of all network parts around the clock.

Our scenarios will focus on investigating effects of electrical faults on the commercial GSM900 and UMTS900 communications network in rural and sub-urban areas where the fault repair takes longer than the provided BS battery backup times; this can happen e.g. due to limited resources and long distances.

The potential fault cases are investigated in substation, recloser and disconnector levels. The studied failure scenarios are:

- Case A: Feeder failure (Earth fault). For example, Earth fault at the remote end in one feeder and recloser in the middle of the feeder trips cuts down electricity from ½ of the feeder.
- Case B: Substation relay failure (more extensive device failure). For example, Fault occurs in a feeder, and substation relay trips causing the entire feeder to go unenergized.
- Case C: Extensive grid failure due to a heavy storm. For example, a heavy storm causes multitude of faults in a defined area (e.g. N faults in 100 km^2), where N is defined by statistical information obtained from typical storms in Finland.

For the simulations, Raasepori area covering 80 km x 60 km was selected as the target area, because both UMTS900 and GSM900 systems are available in that area. The area includes both rural and suburban regions. Exact parameters for the communication or electric distribution networks are not available due to confidentiality constraints. Therefore probabilistic information combined with field-measurements and information from Maanmittauslaitos will be used to make realistic simulations in both urban and suburban areas. The radius of suburban cells is smaller than rural cells, because the suburban cells are assumed to be more capacity limited and rural cells more coverage-limited. The scenarios will include two different terminal heights 1.5 and 3 m. Simulations will be performed both in the DL (BTS→MS) and UL (MS→BTS) directions. Two different types of terminals will be used. A Nemo Handy is used to model a typical mobile terminal for which the commercial network planning is done. Viola System's RTU (GSM or UMTS) is used to model a dedicated Smart Grid communication unit with better antenna gain and lower receiver sensitivity level. The terminals are depicted in Figure 2.

Figure 2. Nemo Handy measurement device was used as typical terminal and Viola System's Arctic EDGE Router and Arctic 3G Gateway for a dedicated RTU.

For the redundancy analysis the following rasters will be computed for coverage, redundancy and interference analysis.

- RSSI
- Dominant cell
- Overlapping cell count
- SNR

4 Simulation model

The simulation model consists of three main parts:

- 3D environment model
- Communication network model
- Electric distribution network model.

4.1 3D Environment model

The environment model consists of a 3D terrain model and a clutter model. Optionally, also building and forest height models can be included. For this project, two 3D terrain models of Raasepori region were constructed based on terrain height and CORINE Land Cover 2006 (CLC2006) information obtained from Maanmittauslaitos (MML) and Suomen ympäristökeskus (SYKE). The clutter layer is constructed from CLC2006 data and it can be presented on the top of the terrain height layer.

A coarse 3D terrain model, presented in Figure 3, has been generated using a triangle mesh, which is constructed from terrain height information with 100 m resolution. It suits well for preliminary calculations and for comparing different statistical propagation models.

Also, a more detailed 3D terrain model, including more precise terrain shapes has been generated. It is based on CLC2006 data with 25 m resolution and its mesh is generated using Delaunay triangulation algorithm. It tries to maximize the minimum angle of all the angles of the triangles in the triangle mesh in order to avoid skinny triangles. This detailed 3D terrain model will be used with profile propagation models, which exploit also information about the changes in terrain height profiles when computing the propagation path loss between a transmitter and a receiver.

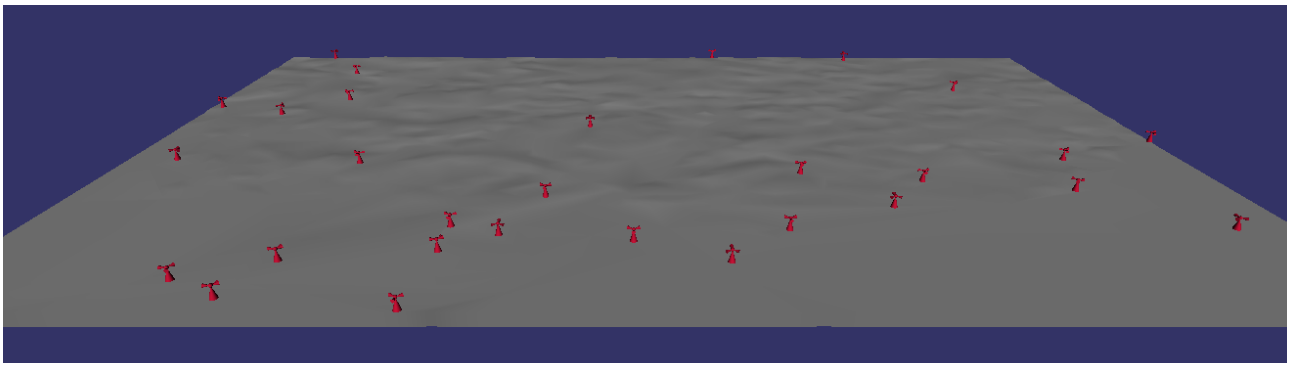

Figure 3. The coarse 3D terrain model.

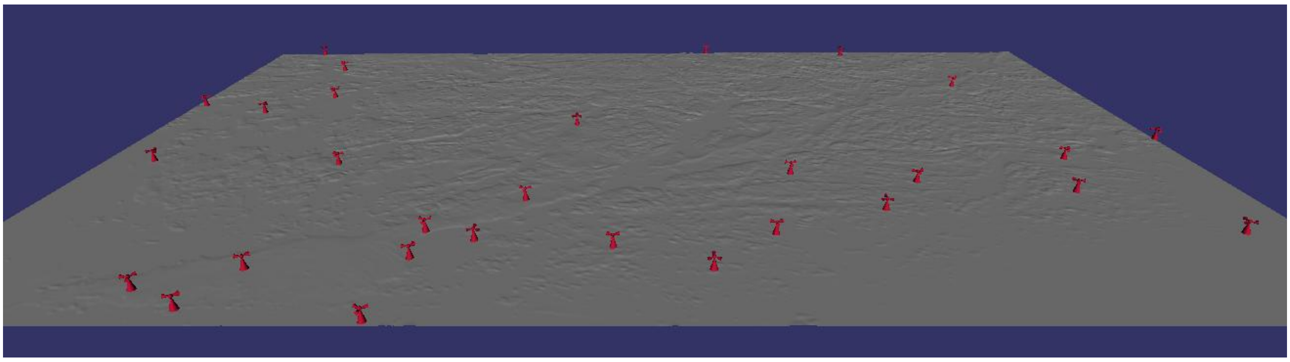

Figure 4. The detailed 3D terrain model.

As mentioned earlier, the clutter model is based on CLC2006 data. The first version of CLC data was completed late 1990's. In year 2000, the CLC database was updated using satellite image of the EU territory (IMAGE2000) to identify main land cover changes in Europe during the period 1990-2000. In CORINE Land Cover 2006 project, the database was updated again (changes in years 2000 – 2006) and high-resolution land cover data as a part of the implementation of the GMES fast track service on land monitoring was produced. The CLC2006 database of Finland is based on automated interpretation of satellite images and data integration with existing digital map data [5].

CLC2006 land cover data describes the land use and soils in Finland. Satellite images were used in estimation of continuous variables describing vegetation type and coverage. Continuous land cover variables are transformed into discrete CLC classes by thresholding these variables according to class descriptions in CLC nomenclature. The classification is three-layered. The first layer includes five main categories [5]:

- artificial surface
- agricultural areas
- forest and open areas
- wetlands,
- water bodies

The second layer contains 15 subclasses and the third layer is divided into 44 classes. Even though the classification is European, all the land use/land cover classes are not included into Finnish data. The Finnish CLC classes are presented in Table 1:

Table 1. CLC classes.

ID	level4	level3	CLC class
1	1110	111	Tiiviisti rakennetut asuinalueet
2	1120	112	Väljästi rakennetut asuinalueet
3	1210	121	Teollisuuden ja palveluiden alueet
4	1220	122	Liikennealueet

ID	level4	level3	CLC class
5	1230	123	Satama-alueet
6	1240	124	Lentokenttäalueet
7	1310	131	Maa-aineisten ottoalueet
8	1320	132	Kaatopaikat
9	1330	133	Rakennustyöalueet
10	1421	142	Kesämökit
11	1422	142	Muut urheilu- ja vapaa-ajan toiminta –alueet
12	1423	142	Golfkentät
13	1424	142	Raviradat
14	2111	211	Käytössä olevat pellot
15	2112	211	Käytöstä poistuneet pellot
16	2220	222	Hedelmäpuu- ja marjapensasviljelmät
17	2310	231	Laidunmaat
18	3111	311	Lehtimetsät kivennäismaalla
19	3112	311	Lehtimetsät turvemaalla
20	3121	312	Havumetsät kivennäismaalla
21	3122	312	Havumetsät turvemaalla
22	3123	312	Havumetsät kalliomaalla
23	3131	313	Sekametsät kivennäismaalla
24	3132	313	Sekametsät turvemaalla
25	3133	313	Sekametsät kalliomaalla
26	3210	321	Luonnonniityt
27	3220	322	Varvikot ja nummet
28	3241	324	Harvapuustoiset alueet , cc <10%
29	3242	324	Harvapuustoiset alueet, cc 10-30%, kivennäismaalla
30	3243	324	Harvapuustoiset alueet, cc 10-30%, turvemaalla
31	3244	324	Harvapuustoiset alueet, cc 10-30%, kalliomaalla
32	3245	324	Harvapuustoiset alueet havumetsärajan yläpuolella
33	3247	324	Harvapuustoiset alueet, käytöstä poistuneet maatalousmaat
34	3310	331	Rantahietikot ja dyynialueet
35	3320	332	Kalliomaat
36	4111	411	Sisämaan kosteikot maalla
37	4112	411	Sisämaan kosteikot vedessä

ID	level4	level3	CLC class
38	4121	412	Avosuot
39	4122	412	Turvetuotantoalueet
40	4211	421	Merenrantakosteikot maalla
41	4212	421	Merenrantakosteikot vedessä
42	5110	511	Joet
43	5120	512	Järvet
44	5230	523	Meri

The land cover and land use information is encoded to a CLC picture as color codes. Thus an additional lookup file is needed to convert picture pixels into land cover and land usage types. The lookup file contains also attenuation factors for predicting the additional propagation loss caused by the land cover and land use types. The lookup table includes also rough height estimate for each clutter type. If a dedicated forest height file is available then more accurate height information can be set for different forest types.

In Figure 5, the 3D environment model from Raasepori region with combined height and clutter information is presented. The red areas illustrate populated areas, light blue ones sea areas, green ones forest and yellow ones open areas. The clutter data is used together with field-measurements. For each clutter type, a correction factor is computed based on measurements. This clutter attenuation information is used to fine-tune the selected propagation model. By default, statistical models do not take into account clutter changes along the propagation path. With the aid of the height and clutter information, the coverage prediction can be made more accurate.

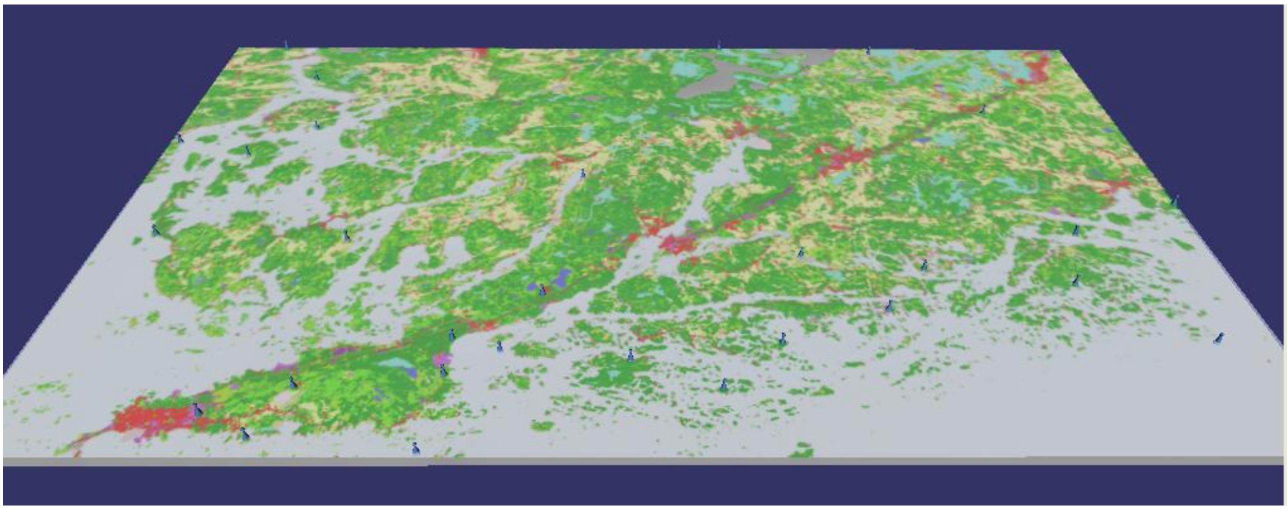

Figure 5. Land cover of Raasepori region.

4.2 Communication network model

The second part of the simulation model is the communication network. Overlapping UMTS900 and GSM900 networks will be constructed using statistical information about average cell density in rural and suburban areas. Additional information about possible mast sites is obtained from TeliaSonera's web page of planned UMTS900 sites [6] and Maanmittauslaitos' map database. The preliminary locations of UMTS900 sites are presented in Figure 6.

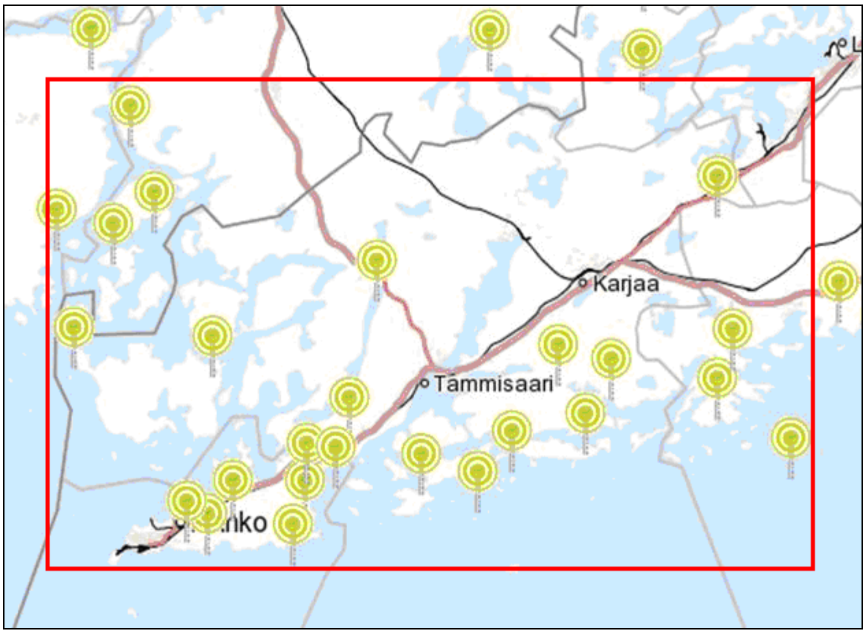

Figure 6. TeliaSonera's preliminary locations of UMTS900 sites in Raasepori region.

The mast sites of Maanmittauslaitos's map database contain all over 60 m high TV, light, or telecommunication masts, or other poles, and such 30 – 60 m high masts, which might obstruct air-traffic. The mast site information was utilized in the creation of GSM900 network.

The simulation tool reads the calculation scenario and respective radio parameters from a configuration file, which is stored in XML format. These configuration parameters are presented as a tree, containing scenario, network, site, terminal, base station and antenna level information. The root level defines the scenario parameters such as the calculation area, resolution, result type as well as the terrain, building, clutter data, and clutter correction term files used in calculations. The second level is the network. It defines radio access technology specific parameters e.g. bandwidth, fading margins, used propagation and clutter calculation models and standard terminal properties. The terminal parameters include information about transmission power, terminal height and antenna specific parameters. The antenna parameters make it possible to model terminal's antenna characteristics very precisely, but for most cases an omni-directional pattern is sufficient. The third level is the site, which defines mast parameters. It contains the mast location and a list of base stations a.k.a cells mounted on it. The fourth level is the base station, which defines the RF parameters of the base station including information about e.g. cell height, transmission power, antenna direction. The fifth level is the base station antenna, which defines antenna parameters such as antenna's radiation pattern, tilt angle and tilt type and cable loss. Typically for base stations, radio access network specific radio pattern files are used. In our simulations, the GSM900 and UMTS900 cells are modeled with 3 sector antennas separated 120° from each other. Kathrein 80010517 antenna pattern was used as a standard antenna for all cells. In Figure 7, the horizontal pattern of Kathrein antenna is shown in the left hand side picture and the vertical pattern in the right hand side picture. Tilting of 1 degree was used in preliminary simulations. The main antenna lobe hits to the ground at the distance of 3 km when the antenna height is 50 m.

Figure 7. Antenna patterns of Kathrein 80010517.

The information presented in the parameter tree is used for calculating the link budget either in the UL or DL direction. The aim is to ensure that the signal transmitted from a transmitter has enough power to be correctly decoded with the desired signal quality at the receiver end. The predicted received power can be computed with the following equations:

$$P_{Tx} + G_{Tx} + G_{Tx,other} - L_{Tx,cable} - L_{PL} + G_{Rx} + G_{Rx,other} - L_{Rx,cable} - R_{SS} - L_{Rx,body} = P_{Rx}$$

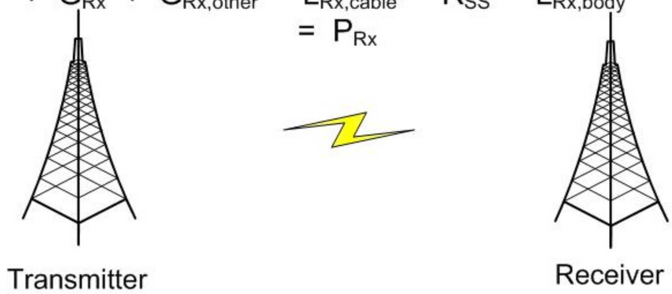

P_{Tx} = transmitted output power (dBm)
G_{Tx} = Tx antenna gain (dBi)
$G_{Tx,other}$ = other Tx gain (MIMO, AAS, diversity) (dB)
$L_{Tx,cable}$ = Tx cable loss (dB)
L_{PL} = path loss (dB)
G_{Rx} = Rx antenna gain (dBi)
$G_{Rx,other}$ = other Rx gain (MIMO, AAS, diversity) (dB)
$L_{Rx,cable}$ = Rx cable loss (dB)
R_{SS} = receiver sensitivity (dBm)
$L_{Rx,body}$ = Rx body loss (dB)
P_{Rx} = received power (dBm)

For the GSM900, calculation frequencies to the DL directions were between 935 – 960 MHz and to the UL directions between 890 – 915 MHz. A simplified frequency planning was performed using values 7 and 1 respectively for the cell cluster size and the frequency re-use distance. For the UMTS900, the center frequencies for DL and UL directions were 942.5 MHz and 897.5 MHz respectively. The radio parameters for the link budget calculations to the UL and DL directions for GSM900 and UMTS900 are presented in the table below.

Table 2. Radio parameters for the link budget calculations.

	Downlink	Uplink
Frequency	GSM900: 935-960 MHz Channels 1-49 UMTS900: Center freq. 942.5 MHz	GSM900: 890-915 MHz Channels 1-49 UMTS900: Center freq. 897.5 MHz
Channel bandwidth	200 kHz (GSM)	200 kHz (GSM)
	Downlink	**Uplink**
Transmit antenna height	30 m (Suburban) 50 m (Rural)	1.5 m (vandal proof case) 3 m (normal case)
Output TX power	43 dBm	23 dBm (EIRP 21 dBm)
Number of TX antennas	3 (Sectored, Kathrein 80010517)	1 (Omni-directional)
Transmit antenna gain & polarisation	4 x 16.7 dBi (Kathrein) (included in rad. pattern)	-2 dBi (GSM) -2 dBi (UMTS900) 6 dBi (3 m height, RTU) 3 dBi (1.5 m height, RTU)
Transmit cable loss	0.4 dB (GSM) 0.4 dB (UMTS900) 29 dB (100m) (RTU)	0 dB
Mechanical tilt angle	1º	1º
Fade margin	10.3	11.7 (Suburban) 10.3 (Rural)
	Downlink	**Uplink**
Number of RX antennas	1 (Omnidirectional)	3 (Sectorial, Kathrein 80010517)
Receiver height	1.5 m (vandal proof case) 3 m (normal case)	30 m (Suburban) 50 m (Rural)

Receiver antenna gain & polarisation	-2 dBi (GSM) -2 dBi (UMTS900) 6 dBi (3 m korkeus, RTU) 3 dBi (1.5 m korkeus, RTU)	4 x 16.7 dBi (Kathrein) (included in rad. pattern)
Receiver cable loss	0 dB	0.4 dB (GSM) 0.4 dB (UMTS900) 29 dB (100m) (RTU)
Receiver noise figure	10 (GSM), S/N 9 dB 9 (UMTS900)	2.5
Receiver sensitivity	-102..-104 dBm (GSM) -108 dBm (UMTS900) -100 dBm (RTU)	-112 ... -114 dBm (GSM) -120 dBm (UMTS900) -120 dBm (RTU)

4.3 Electric distribution network model

Smart Grids, which are fundamentally the integration, by control and communication, of all power system elements, will rely upon effective communications technology and infrastructure throughout the electric power system. Most utilities do not have communications throughout their service territory. Typically, they may have some communications in their substations, likely wireline, and they may have a land mobile radio and multiple address system for SCADA data, all on a highly-limited, private network. The Smart Grids require communications to all devices throughout a service territory, including meters, feeder automation devices and distributed generation assets. Network infrastructures for the Smart Grids are digital, capable of two-way communication, designed to be highly reliable. The Smart Grids enable active participation of consumers by connecting them to their consumption of electricity through relevant modern technology [7].

In our model, we are focusing on the medium-voltage components of the electric distribution network namely substations, recloser and disconnectors, which operations can be automated and remotely controlled over a wireless link. The model is presented in Viola Systems' white paper [8].

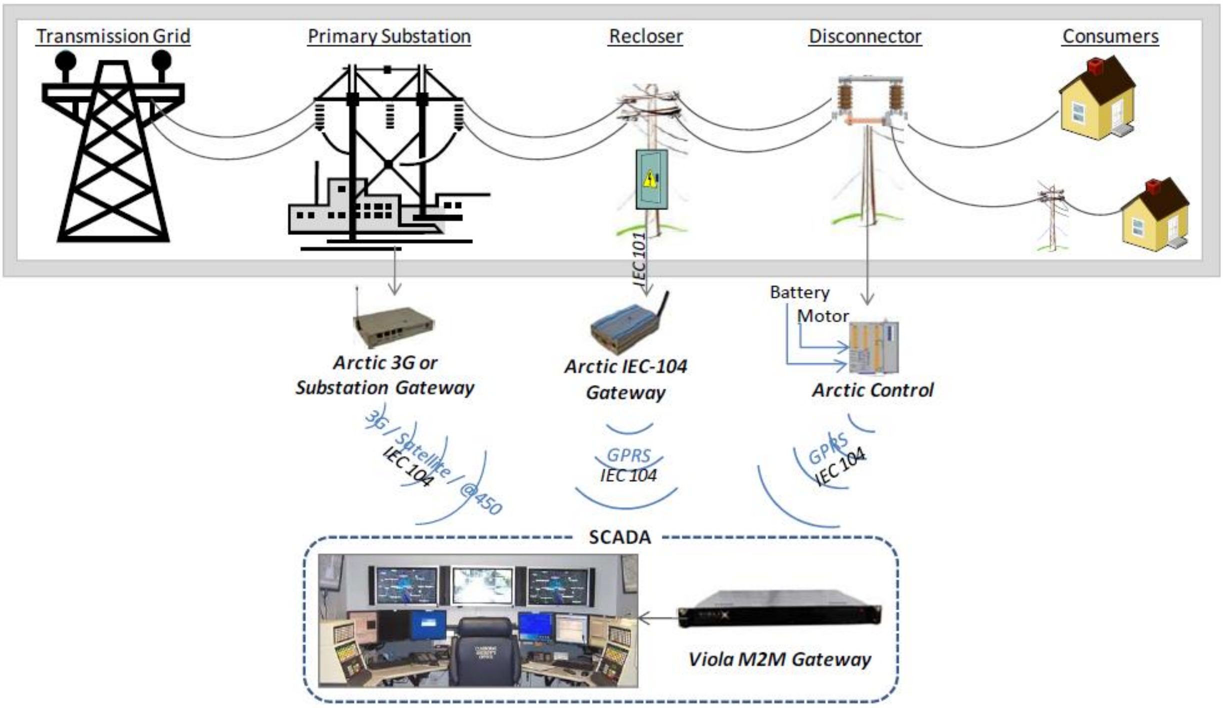

Figure 8. Visualization of Vattenfall's Smart Grid solution [8].

For smart grid operations, Viola Systems has a product family [8] that is capable of utilizing 2G and 3G networks in order to

- provide a continuous connection based on wireless, IP based technology leveraging cellular networks
- provide automatic connection monitoring and re-establishment in case of communication failure
- reserve large communication capacity to retrieve additional monitoring information from the electric distribution network

Ultimate justification for the DSO of investing into feeder automation is to minimize customer interruption related penalties as stipulated by the regulator [6]. The feeder automation (FA) concept will be summarized in the following. For details refer to [17,18].

A MV distribution network contains substations, reclosers and disconnectors having their specific responsibilities:

Substation [9] transforms voltage from high to low, or vice versa. Electric power usually flows through several substations between power plant and consumer, and its voltage changes in several steps. Electrical distribution networks have primary substations, which are connected to the high voltage grid. Such primary substations have multiple medium voltage feeders, which distribute the electricity to customers.

Recloser [10] is used to dividing the distribution network into smaller sections. As a result, a single failure event on the grid will cut off only the section controlled by the recloser. Because resetting a breaker might take considerable time, reclosers are used to automatically re-connect after a short interval. About 80-90% of faults on overhead power lines is transient and can be cured by autoreclosing. Reclosers can break fault currents.

The following figure shows an example of a pole mounted recloser as used along the MV feeder

Figure 9. An example of a MV feeder with a recloser (ABB picture).

Disconnectors [11] are used along the MV network to re-configure the feeder topology with the aim to isolate faults to a relatively small control zone. They are also used to close normally open (N.O.) points to allow alternative power feed-in from another substation. Disconnectors are not rated to break fault currents. The following figure shows an example of a remote controlled disconnector station along the MV feeder.

Figure 10. An example of a MV feeder with a disconnector (ABB picture).

Each of these entities has their own operational zones forming a hierarchical structure illustrated in Figure 11. The uppermost level is the service area, which is divided into smaller substations zones.

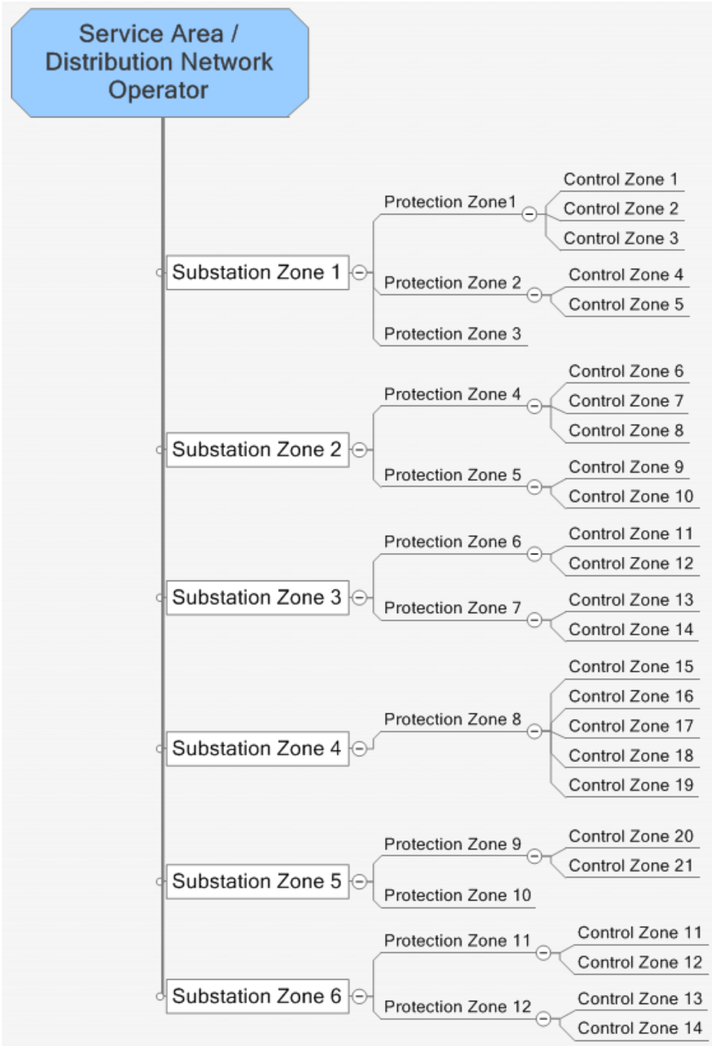

Figure 11. An example of the hierarchy of substation, protection and control zones.

The substation zone is a geographical area to which the substation supplies the electricity. Reclosers and/or load break switches divide substation zones into protection zones. When a failure occurs in the middle of a protection zone, the faulty protection zone gets isolated automatically. Disconnectors (or RMU or other type of switch) divide protection zones into smaller control zones. When a failure occurs in the middle of a control zone, the faulty protection zone can be remotely isolated from the Scada system. The following figure illustrates one substation zone having two protection zones.

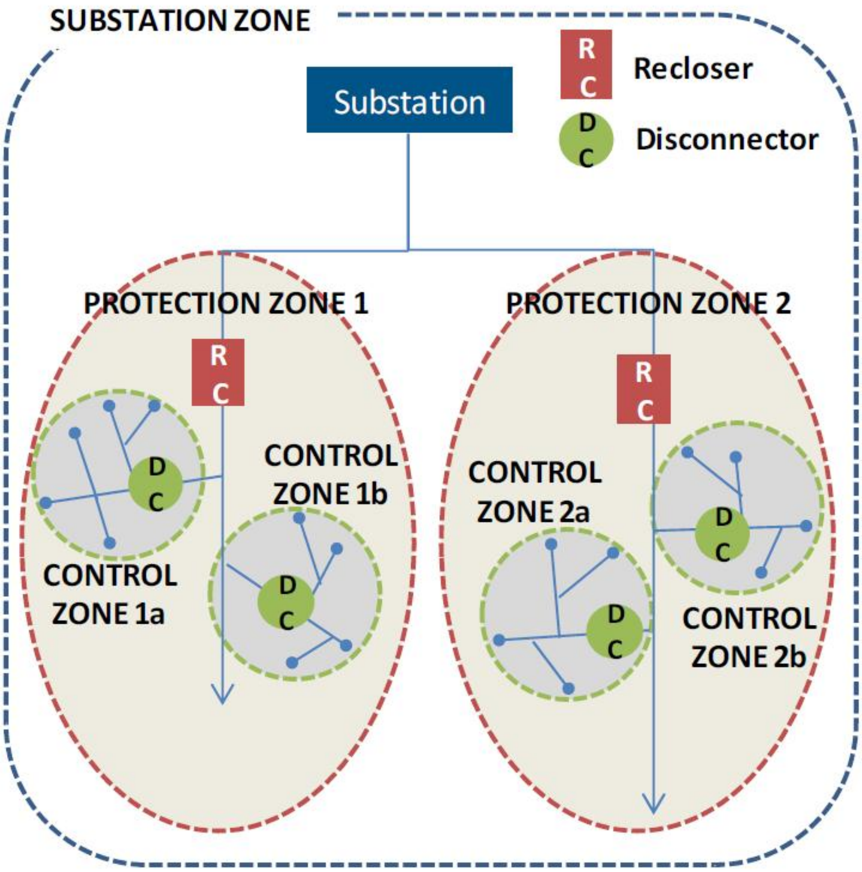

Figure 12. An illustration of the zone concept from [8].

To be more precise, reclosers have programmable off-on switching sequences which aim at arc extinction of transient faults. A first, short duration HSR (High Speed Reclosure) aims at cooling the arc sufficiently to clear temporary faults such as arcs triggered by lightening strokes. If not successful, the HSR is followed by a longer duration DR (Delayed Reclosure) for burning off e.g. tree branches or small animals causing short circuit conditions. If the DSR fails, then the fault is called permanent and it needs to be localized and isolated by operating remote controlled disconnectors.

Relays at the reclosers can measure (fault) currents and this information, when transmitted to SCADA/DMS, can assist DMS to find the location of the fault (e.g. by using an equivalent impedance estimate). Another, more time-consuming method is to remotely and manually open and close disconnectors until the fault is isolated and the re-closer doesn't break fault currents any longer. Unlike disconnectors, reclosers are designed to break the larger fault currents. For fault isolation into a control zone, disconnectors must therefore be operated with the closest upstream recloser having cut power off. Reclosers and disconnectors always report their switching state (on/off) to SCADA. Having a consistent picture of the current switching state at SCADA/DMS is the most important driver for increasing reliability of the communications.

Not shown in the above figure are the relays at the substation feeder termination. Their respective settings are coordinated with the settings of the feeder re-closers in such a way, that the feeder recloser activates for downstream faults always before the substation's recloser. With the above arrangement, a fault downstream of re-closer in zone 1 would not impact customers upstream or in protection zone 2. This applies also for HSR and DR attempts, which also lead to penalties for the DSO. The following figure from [20] shows statistics for the re-closing success rates in rural, suburban and urban regions.

7.1 Pika- ja aikajälleenkytkentöjen selvittämät viat kaikista vikakeskeytyksistä

	Maaseutu	Taajama	City
PJK:n selvittämät viat	53%	43%	13%
AJK:n selvittämät viat	23%	18%	14%
Pitkät keskeytykset	24%	39%	73%

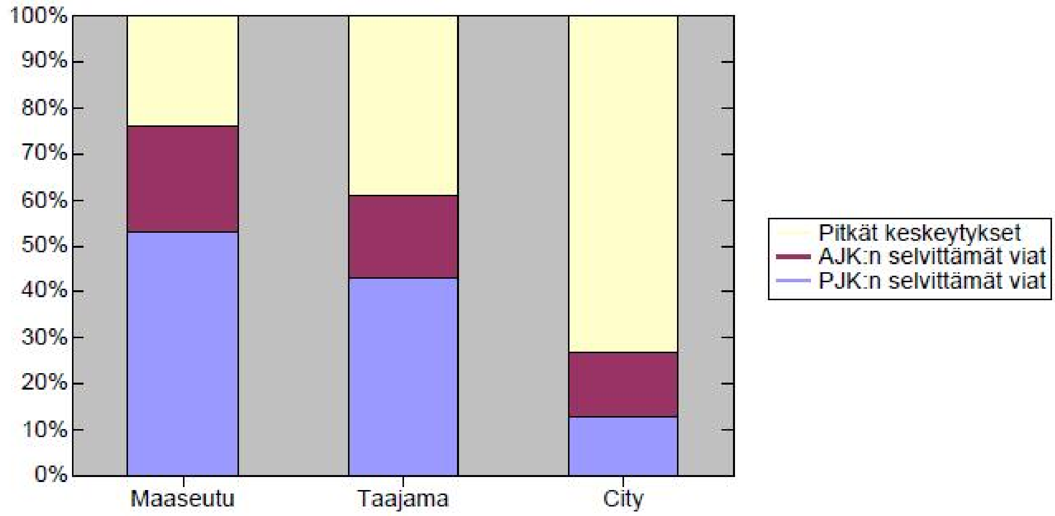

Figure 13. Statistics for the re-closing success rates in rural, suburban and urban regions.

Finally, for illustration, the following figure shows an example of protections and control zones in parts of the FORTUM MV network in Masala region.

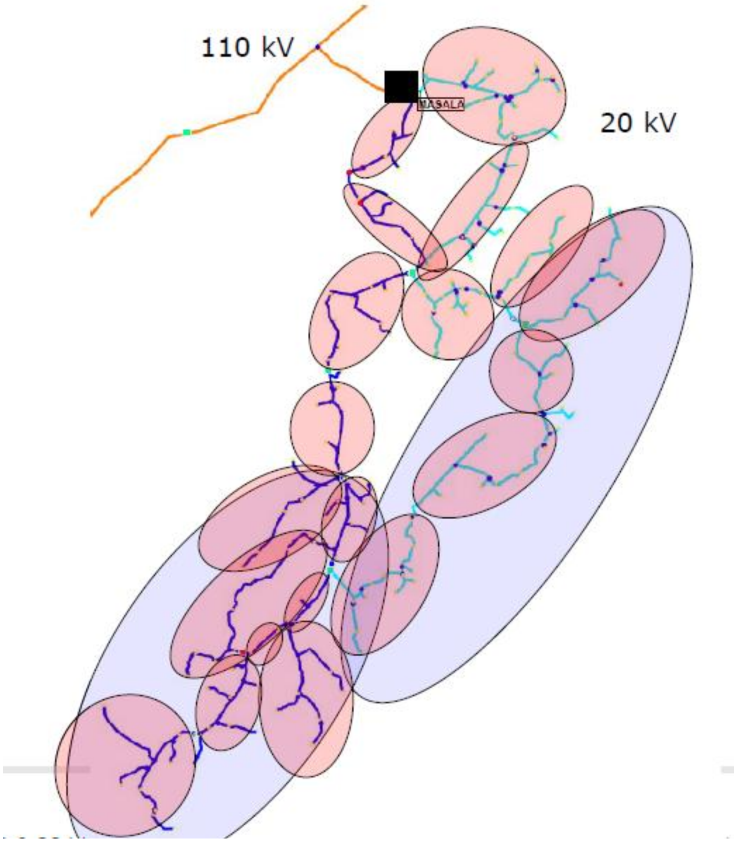

Figure 14. Fortum's MV network in Masala region.

Based on the physical model of an electric distribution network, a simulation model was designed. The simulation model, shown in Figure 15, was based on composite design pattern [12], which enables to create complex tree and graph structures. The uppermost layer is distribution network that models the distribution network at the given region. The network contains one or more service areas. Each service area can include one or more service areas, primary/secondary substations, disconnectors, reclosers, feeders and BTS connectors. Under one substation, there can again be one or more electric distribution entities. A BTS connection can only contain one entity, which refers to a link between an electric distribution entity and a base station mast. The link is created using the shortest distance algorithm. Through BTS connections, specific communication masts and their cells are forced to switch off in simulations. Each electric distribution network entity has its own operational zone. The shape of the zone can be a rectangle, circle, polygon or polyline.

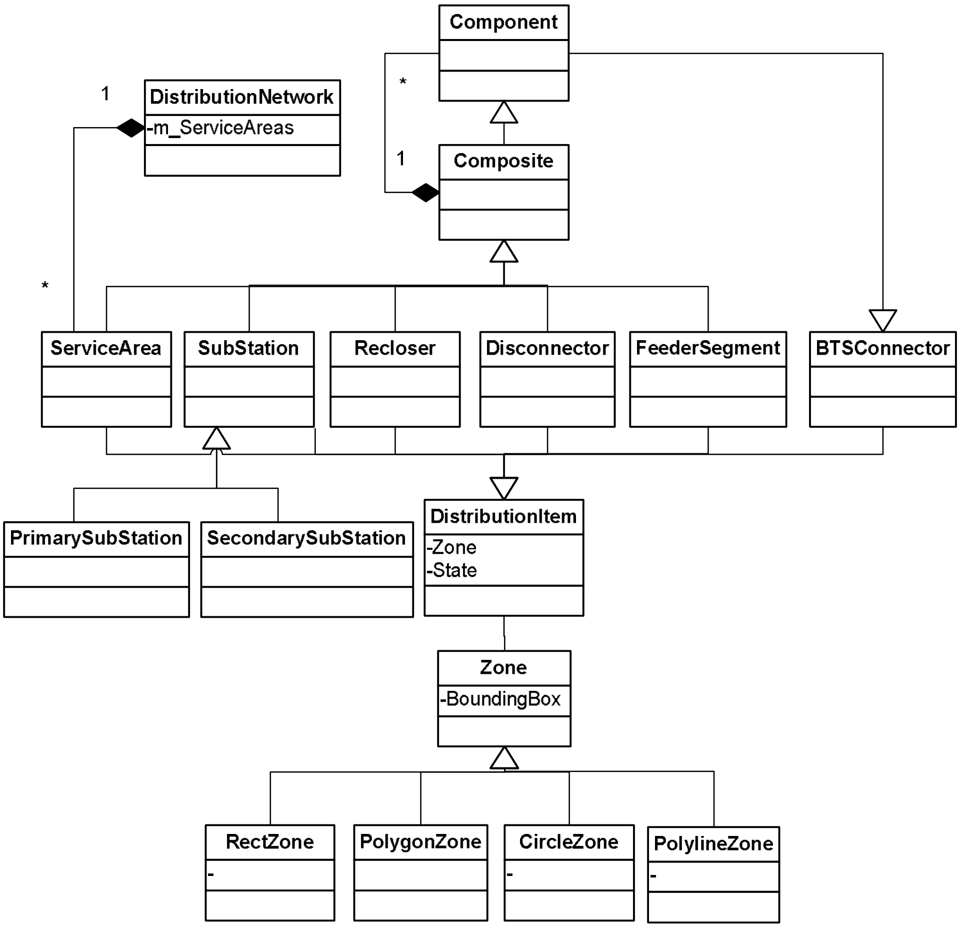

Figure 15. A class diagram of simulation model.

There are roughly 20 primary substations, 80 feeders, 50 disconnectors and approximately 1400 secondary substations modeled in Raasepori area based on the input obtained from ABB and Fortum. **Figure 16** shows the generated secondary substation network where colors are indicating different feeders. The locations of primary substation or feeders segments were not available. Thus the area of a feeder is created using the locations of secondary substations associated with it. The land texture is removed from the picture in order to make feeder regions more visible.

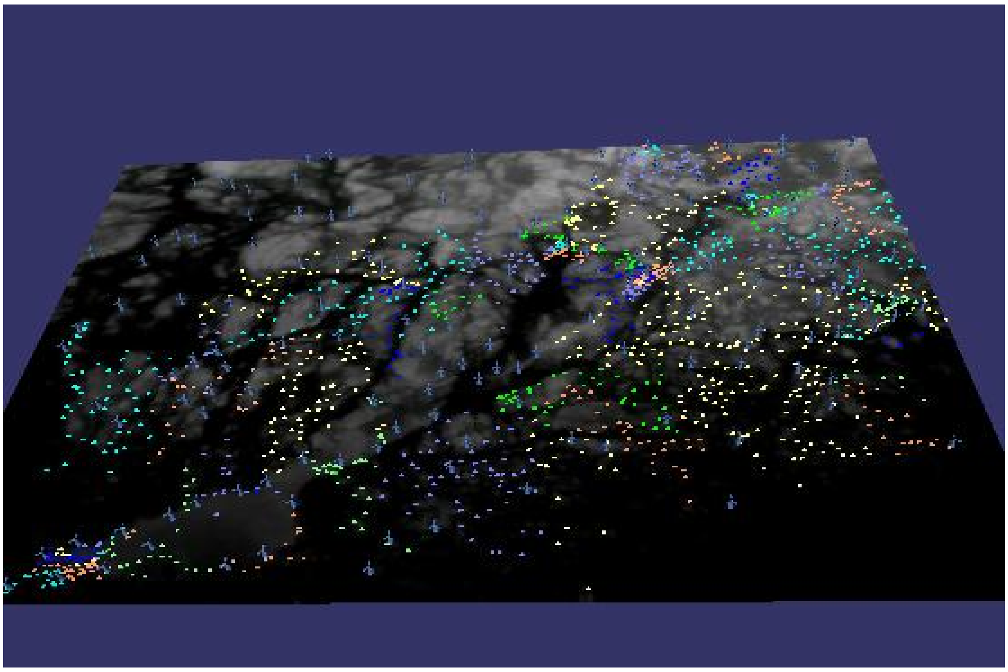

Figure 16. Locations of secondary substations in Raasepori area.

Figure 17 shows the GSM900 masts that are connected to the closest secondary substation. In the figure, the green colour indicates that the power of the mast is on.

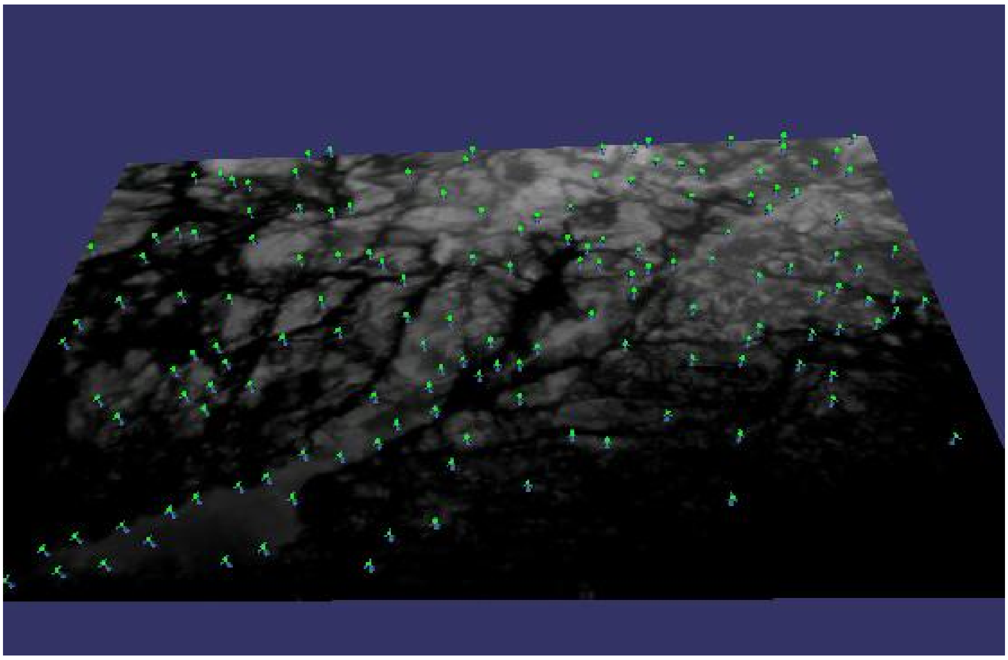

Figure 17. Locations of GSM900 masts in Raasepori area.

During the simulations, failures are generated in primary substation, feeders and part of the feeder level. As a result, the corresponding secondary substations get de-energized and consequently also those masts connected to them. When the mast is de-energized, the GSM900 cells mounted on the mast stop transmitting (assumed that the fault time exceeds the backup battery time) and the coverage and inherent redundancy starts deteriorating.

4.4 Model fine-tuning with field measurements

The locations or RF parameters for UMTS900 and GSM900 networks were not available due to confidentiality constraints. As a result, these networks were generated and parameterized using prior knowledge, literature surveys and input from SGEM partners. In order to get some level assurance of prediction accuracy, a measurement trial was performed in Raasepori on 11.11.2011 by VTT and Viola Systems. The measurement included two drive measurements and 10 stationary measurements. The measurement data was collect from GSM900 and UMTS900 networks for propagation model tuning and for assessing the performance of a typical commercial mobile terminal equipped with an internal antenna, and a RTU terminal equipped with an external antenna.

During the drive measurements, only GSM900 network was measured. The Nemo Handy device was continuously measuring different performance parameters from serving and neighbouring GSM cells. During the first drive measurement, the car was stopped approximately every 8 – 10 km and a stationary measurement was performed with Viola System's Arctic EDGE Router (GSM900) and Arctic 3G Gateway (UMTS900) devices.

Figure 18. The car used for measurements. The RTU's external antenna is mounted on the middle of the car roof.

During the second drive measurement the Nemo Handy was locked on one cell. The measurement was done to give a rough estimate about the radius of a GSM900 cell in rural/suburban area. The car was driven first towards the mast and then away from it until the connection was lost. By locking on one channel, the Nemo Handy was prevented from leaving the cell until the signal was under the reception threshold. The parameters measured by a Nemo Handy are presented in table below. For propagation model tuning, the main interest was in RxLev full values of serving and neighboring cells.

Table 3. GSM measurement report [14].

Name	Description
Cell type	Number of parameters per cell Cell type Integer Cell type 0 = Neighbor 1 = Serving
Band	Band 10850 = GSM 850 10900 = GSM 900 11800 = GSM 1800 11900 = GSM 1900 19999 = GSM
ARFCN	Channel number
BSIC	Base station identification code
RxLev full	RX level full. The received signal level of all TDMA frames. See 3GPP TS 145.008 subclause 8.4.
RxLev sub	RX level sub. The received signal level of the subset of the TDMA frames. See 3GPP TS 145.008 subclause 8.4.
C1	Path loss criterion parameter C1 is used for cell selection and re-selection. See 3GPP TS subclause 6.4 (with GPRS, also subclause 10.1.2).
C2	The reselection criterion C2 is used for cell reselection. This parameter is used for cell reselection when the value of the path loss criterion C1 is over zero. See 3GPP TS subclause 6.4.
C31	The signal level threshold criterion parameter C31 is used to determine whether prioritized hierarchical GPRS and LSA cell re-selection shall apply. See 3GPP TS 145.008 subclause 10.1.2.
C32	The cell ranking criterion C32 is used in selecting cells from cells that have the same priority. See 3GPP TS 145.008 subclause 10.1.2.
HCS priority	HCS priority class. Defines the cell re-selection order of the cells. See 3GPP TS 145.008 subclause 10.1.3.
HCS thr.	HCS threshold. See 3GPP TS 145.008 subclause 10.1.2.

Cell ID	Cell identification. Cell identification of the serving cell.
LAC	Location area code
RAC	Routing area code
Srxlev	Neighbor Srxlev S criteria (based on RX level). This value is only available during the UMTS mode

4.4.1 Measurement of locked channel

The locked channel measurement was used to estimate the average cell size and optimize the effect of land cover in propagation models. The Nemo Handy was locked on one of the GSM900 cells placed on a high mast shown in Figure 19. The mast is located next to the road and its location was estimated accurately enough with a digital map and visual perception. The RF parameters of the selected cell were not known.

The measurement was started from a gas station shown in the middle of Figure 19. First, the car was driven northwest towards the mast and after passing it, a U turn was made. Then, the car was driven southeast past the gas station until the connection was lost. The total length of the route was 13 km. The route with received RX levels is presented in Figure 19 and Figure 20. The warmer (orange) colours indicate higher RxLev values.

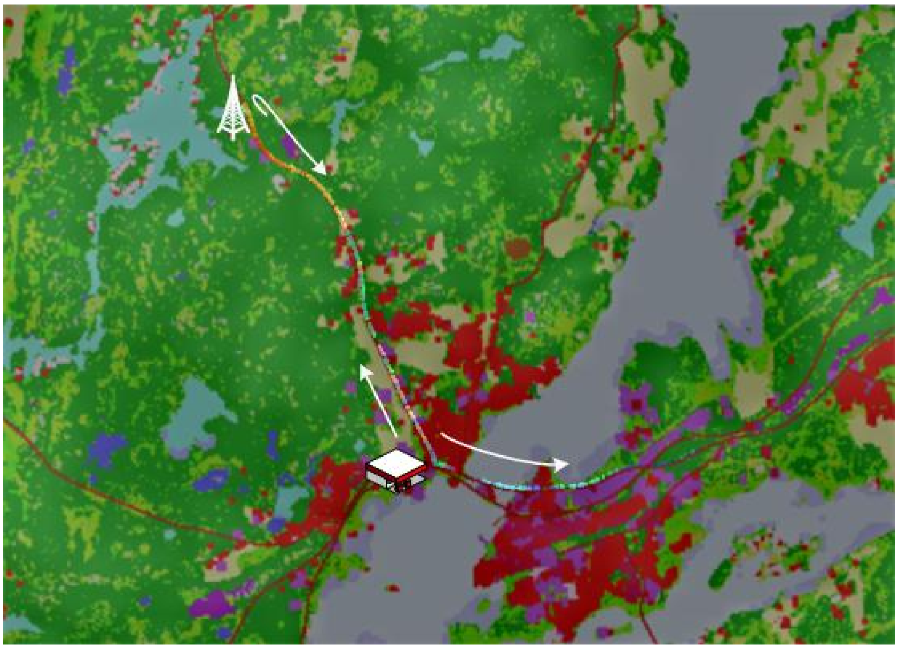

Figure 19. Short measurement route in Raasepori.

Figure 20. Signal strengths of serving cells along the measurement route.

Figure 21 shows the received signal strength along the measurement route. From the figure, we can see that there occurs a short communication break just before the car enters the bridge. This break is caused by terrain and buildings hindering the communication link. This can be observed by examining the terrain height graph in Figure 22. The connection is totally lost when the car is about 6.5 km from the mast.

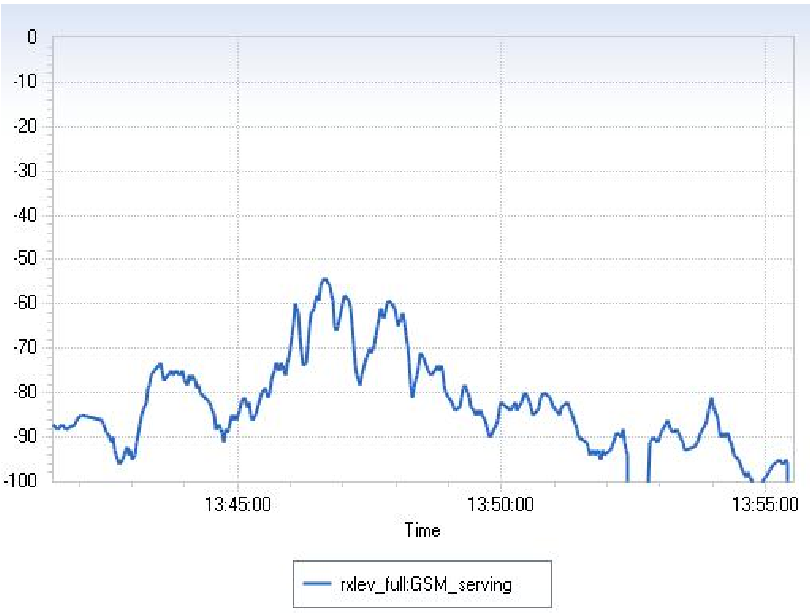

Figure 21. Signal strengths of serving cells along the measurement route.

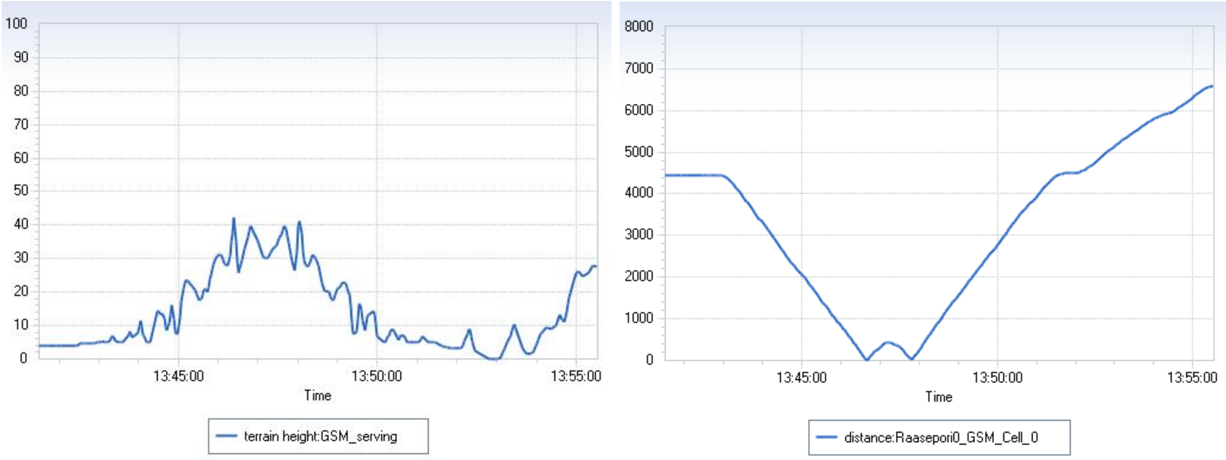

Figure 22. Terrain heights and the distances from the mast.

4.4.2 Measurement of locked system

The measurement was done by locking the Nemo Handy to the GSM900 system. The route is presented in Figure 23 and Figure 24. The measurement route resembles number eight and it was about 94 km long. The measurement was started from the same gas station as in case of the channel locked measurement. The colour values presented in Figure 23 and Figure 24 are indicating the received signal strength of the serving cell. The measurement data includes also information about the neighbouring cells. Along the route, 74 GSM900 cells, who's Cell ID could be deduced from the measurement, were found.

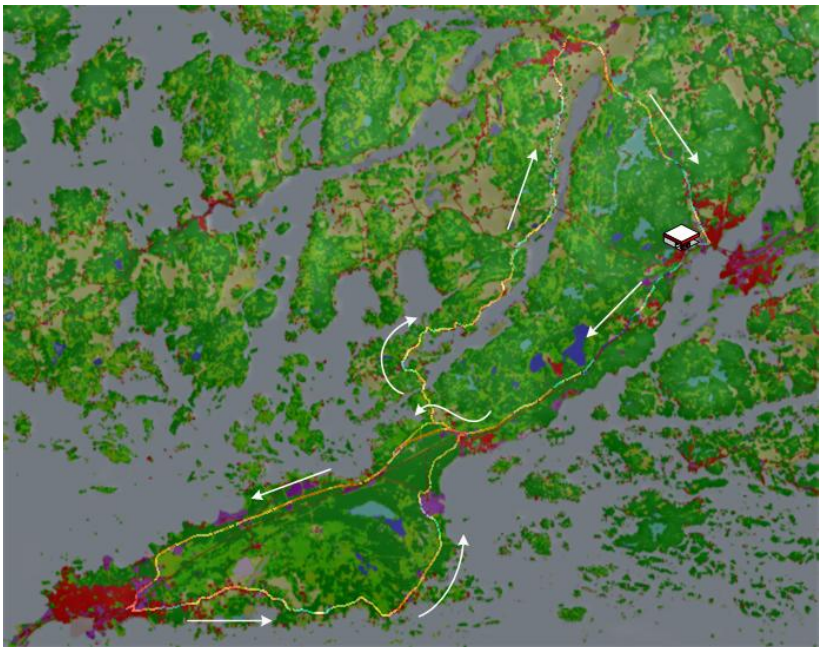

Figure 23. Long measurement route in Raasepori and Hanko.

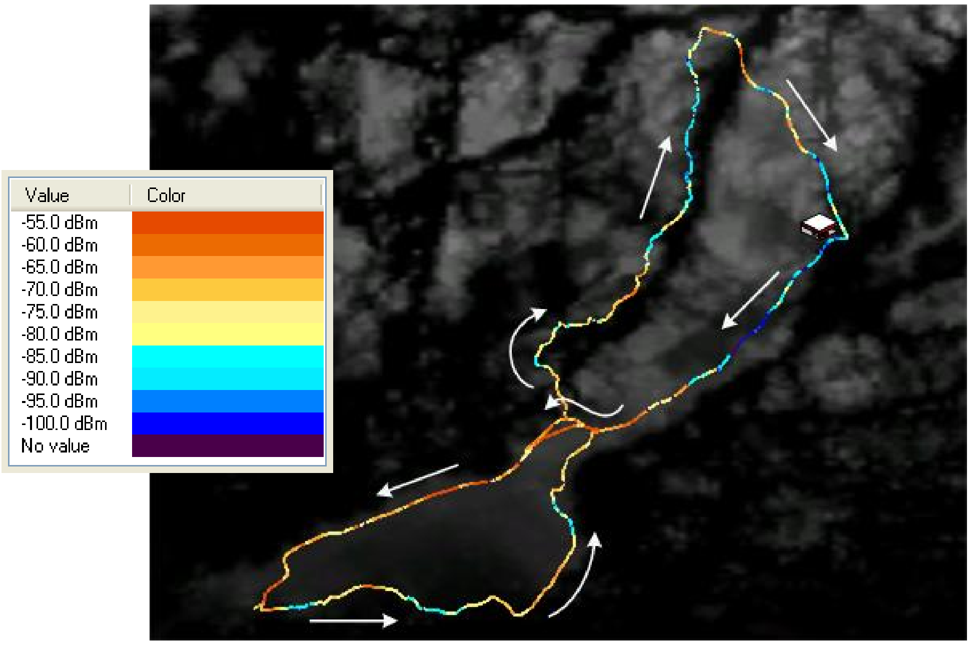

Figure 24. Signal strengths of serving cells along Raasepori and Hanko route.

Figure 24 shows the received signal strength along the measurement route. The signal strength is rather low (dark blue) in the beginning and in the end of the route. The value is below -85 dBm (read from Figure 25).

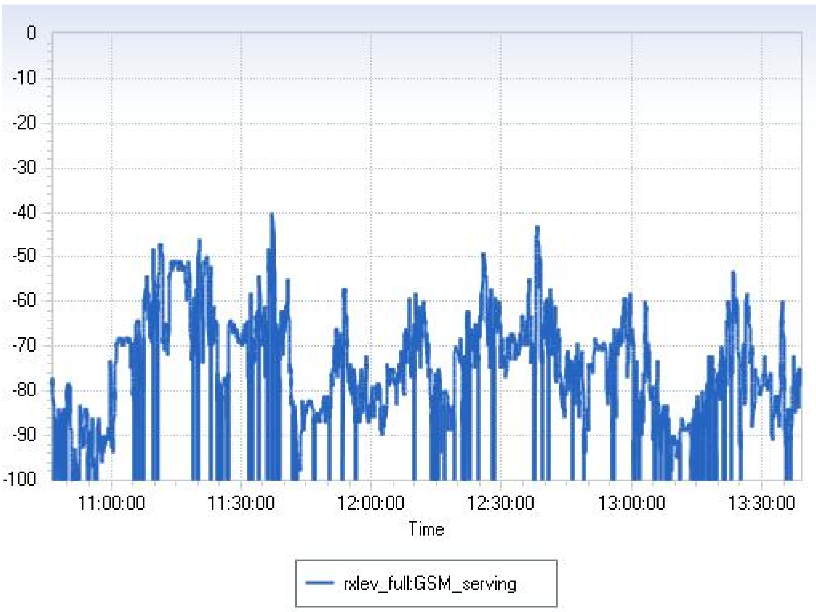

Figure 25. Signal strengths of serving cells along the long measurement route.

The GSM terminal reports only six best neighboring cells. Therefore, the upper limit for measured cell count is seven (serving cell + 6 neighboring cells). When we look at the cell counts along the measurement route, presented in Figure 26, we discover that those areas having low serving cell's signal strength values are also those having low cell count values.

Figure 26. Cell counts along the long measurement route.

4.4.3 Stationary measurements

The stationary measurements were carried with Viola Systems UMTS and GSM measurement devices in ten locations. These locations are shown in Figure 27. Measurement points 2 and 7 were accidentally chosen to be next to each other. During these stationary measurements also the Nemo Handy terminal was kept measuring in order to collect data for the performance comparison of a Nemo Handy terminal with an internal antenna and Viola System's RTU with an external antenna.

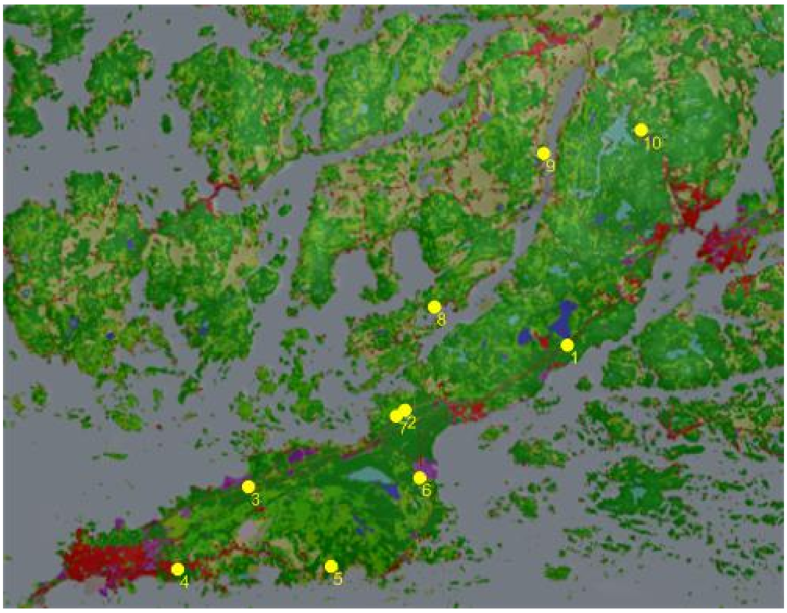

Figure 27. Locations of stationary measurements.

The measured RX level values with a RTU and a Nemo Handy terminal are presented in Figure 28 in different locations. The RTU's average RxLevel value is shown with a red line labelled as RTU, and values measured with the Nemo Handy over the time period are shown with a blue line. The Nemo measurement includes all the measured samples that were measured within 10 meters from the reference location. The gaps in the graphs are likely to be resulted from GPS errors, which increased the distance between the location of a Nemo measurement sample and the reference point over 10 meters. The variations in values are likely to be resulted from the change of the serving cell. Nevertheless, the fluctuation in the Nemo Handy results is such that further analysis and additional measurements are needed.

Reference point #1

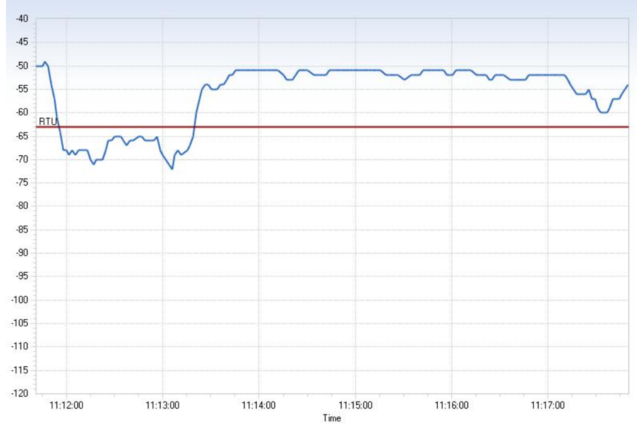

Reference point #2

Reference point #3

Reference point #4

Reference point #5

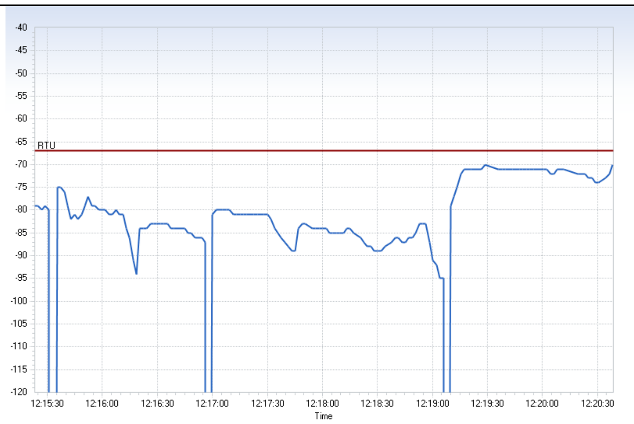

Reference point #6

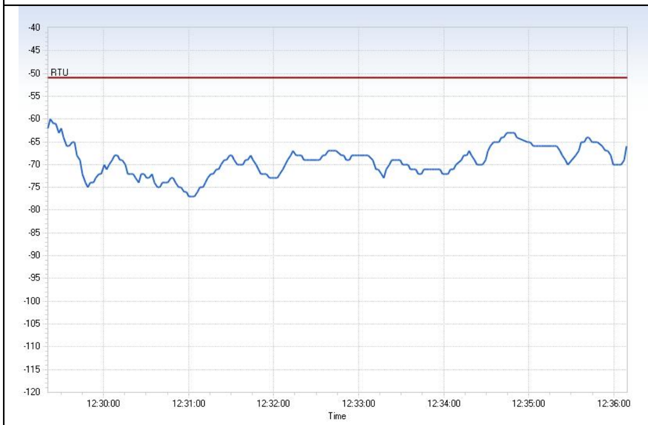

Reference point #7

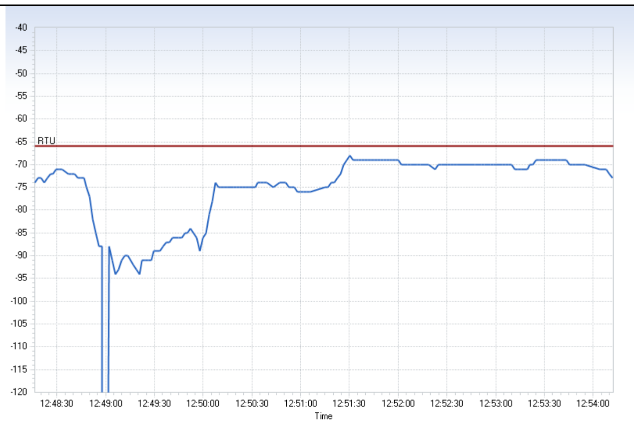

Reference point #8

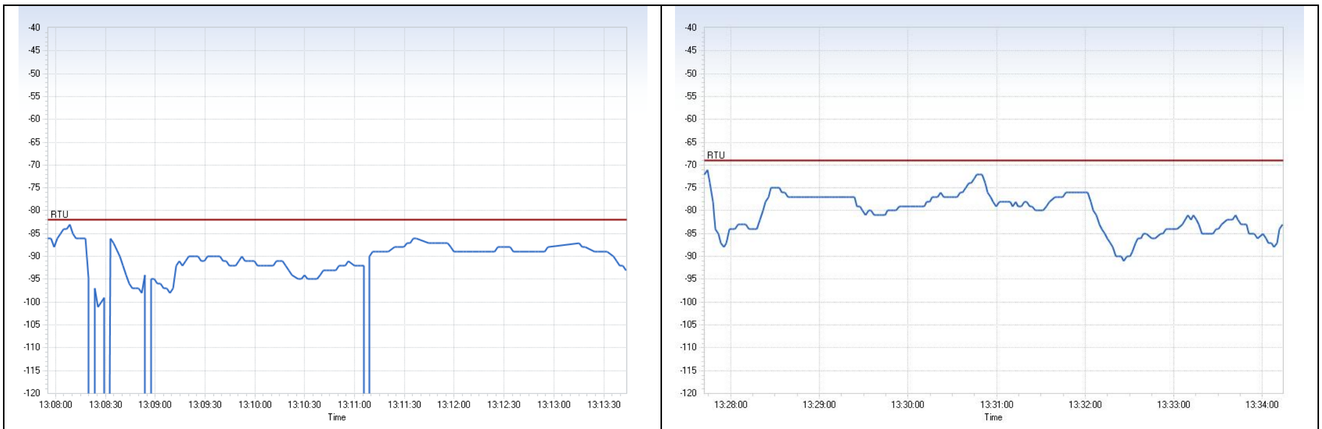

Reference point #9

Reference point #10

Figure 28. Measured Rx level values in 10 reference points.

The next figure shows the number of 'hearable' cells with different measurement devices. The Nemo's cell count exceeds the maximum number of cells that the GSM terminal can report at one time. Since the measurement period was rather long, the Nemo terminal was switching the serving cell. As a result, more cells either serving or neighbouring were recorded. The interesting result is that the average cell count for GSM900 measured with Arctic Edge Router is above four, but for the UMTS900, only one 'hearable' cell was obtained with Arctic 3G Gateway at each reference point. This is likely to be a measurement device related constraint. Nevertheless, this requires further investigation. More detailed analysis of Viola Systems' stationary measurements is presented in a technical report [13].

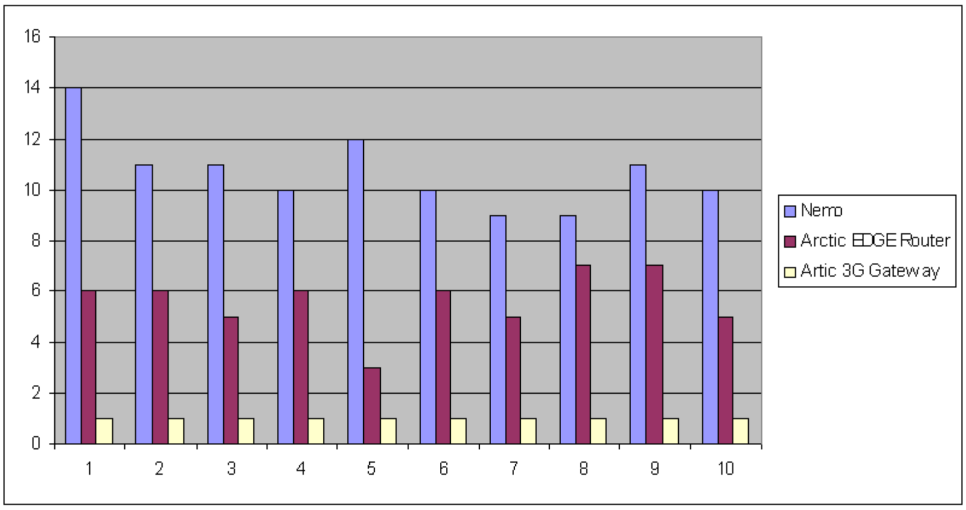

Figure 29. Cell counts with different measurement devices.

4.5 Coverage and redundancy assessment

The starting point for simulations was to select a suitable propagation model. Different propagation models were evaluated with the specified base station and terminal heights and transmission powers. The calculation area is so large that the evaluation was limited to statistical models. Longley-Rice and CCRHata gave the best results (clutter corrections were not used), and thus were selected for the analysis.

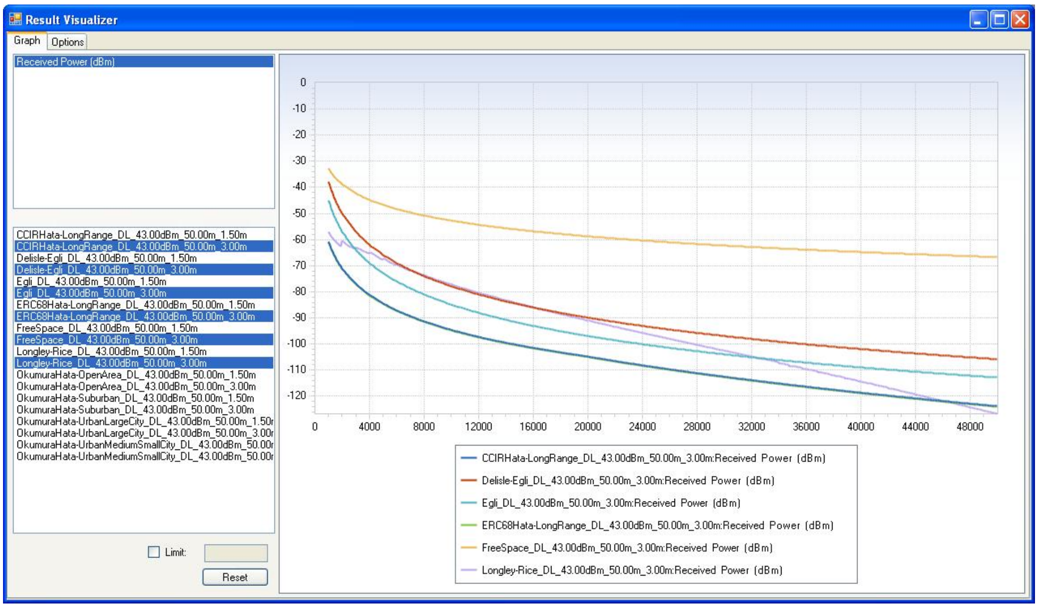

Figure 30. Link budget for GSM900 using 43 dBm transmission power, 50m antenna height, and 3 m terminal height.

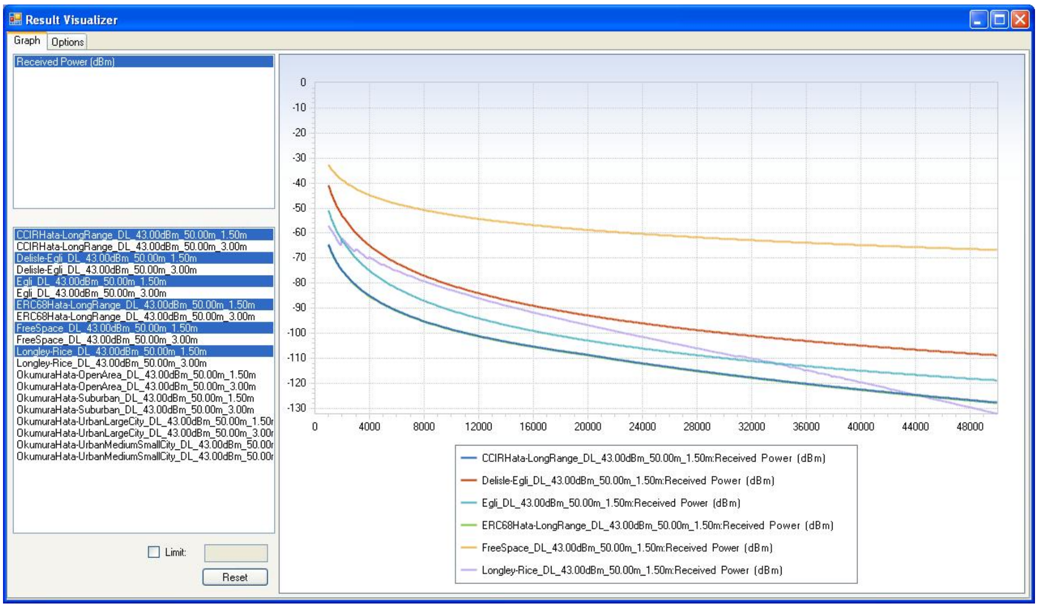

Figure 31. Link budget for GSM900 using 43 dBm transmission power, 50m antenna height, and 1.5 m terminal height.

4.5.1 Propagation model calibration

Results from the short measurement were used to compute clutter correction terms to the propagation models. The pictures below (see Figure 32) show the effect of propagation model tuning. The first set of pictures shows the results when no clutter correction or model tuning was applied. The RxLev graph indicates that the CCIRHata (long range) propagation model is underestimating the attenuation near a base station and overestimating it at longer distances. Since the properties of the base station were not known, it is also possible that the antenna sector settings (e.g. direction of the antenna, radiation pattern or tilting) were not accurate enough.

When we look at the results after the first tuning with measured data, the predicted and measured values correspond to each other. The optimisation corrects the average RxLev level as well as some inaccuracies caused by the environment. But, the drawback is that the coverage raster computed with these correction terms looks a bit uncharacteristic and granular. Some of the terms are amplifying the received signal too much. This is the consequence of using data from only one short measurement route. As a result, all the clutter types weren't found and the number of samples of specific clutter types was too low to give the best possible optimisation result. For better result, the measurement route should have been made longer or the same measurement should have been repeated several times. In FP3, more measurements are planned to be carried out.

To make clutter terms more realistic, we fine-tuned the optimised coefficients by hand. After the fine-tuning, there exist more deviations between predicted and measured values. This is shown in the third picture set. The reason is that there are still too many inaccuracies in base station parameters and environment modelling. The optimisation cannot compensate all those errors. For example, the attenuation from buildings is not modelled accurately enough. Only few clutter types are specified for built environments. The statistical CCIRHata (long range) propagation model overestimates the average propagation loss along the route, so after manual fine-tuning the calculation result ends up being more pessimistic than the measurement.

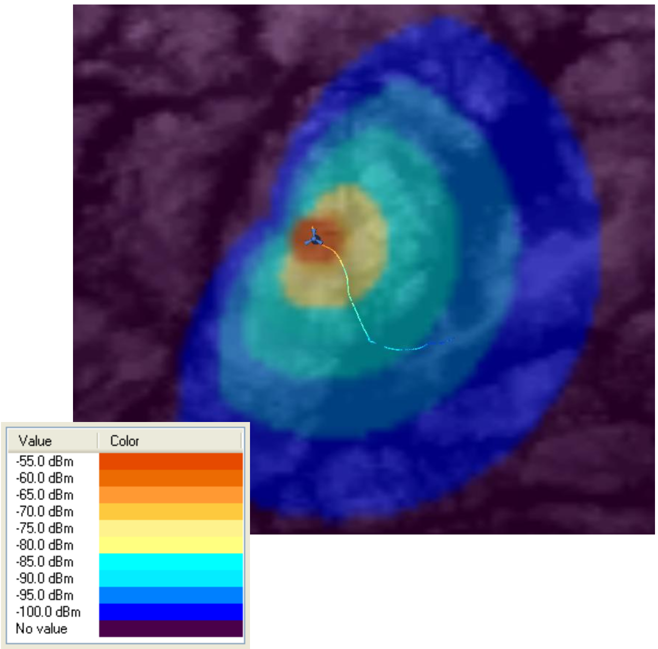

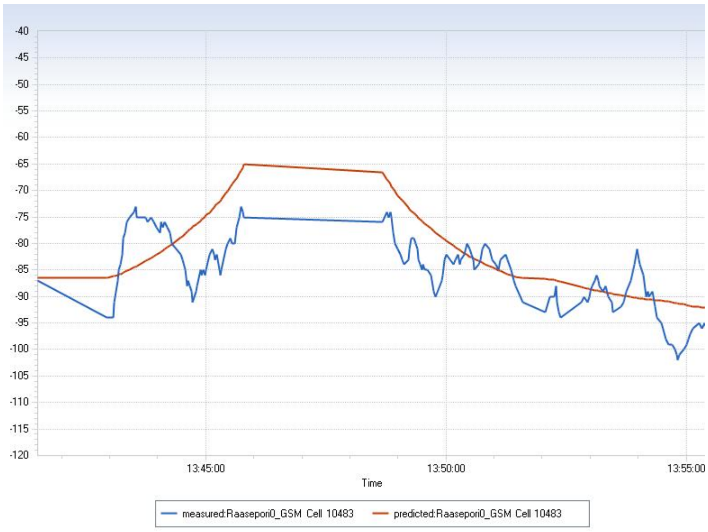

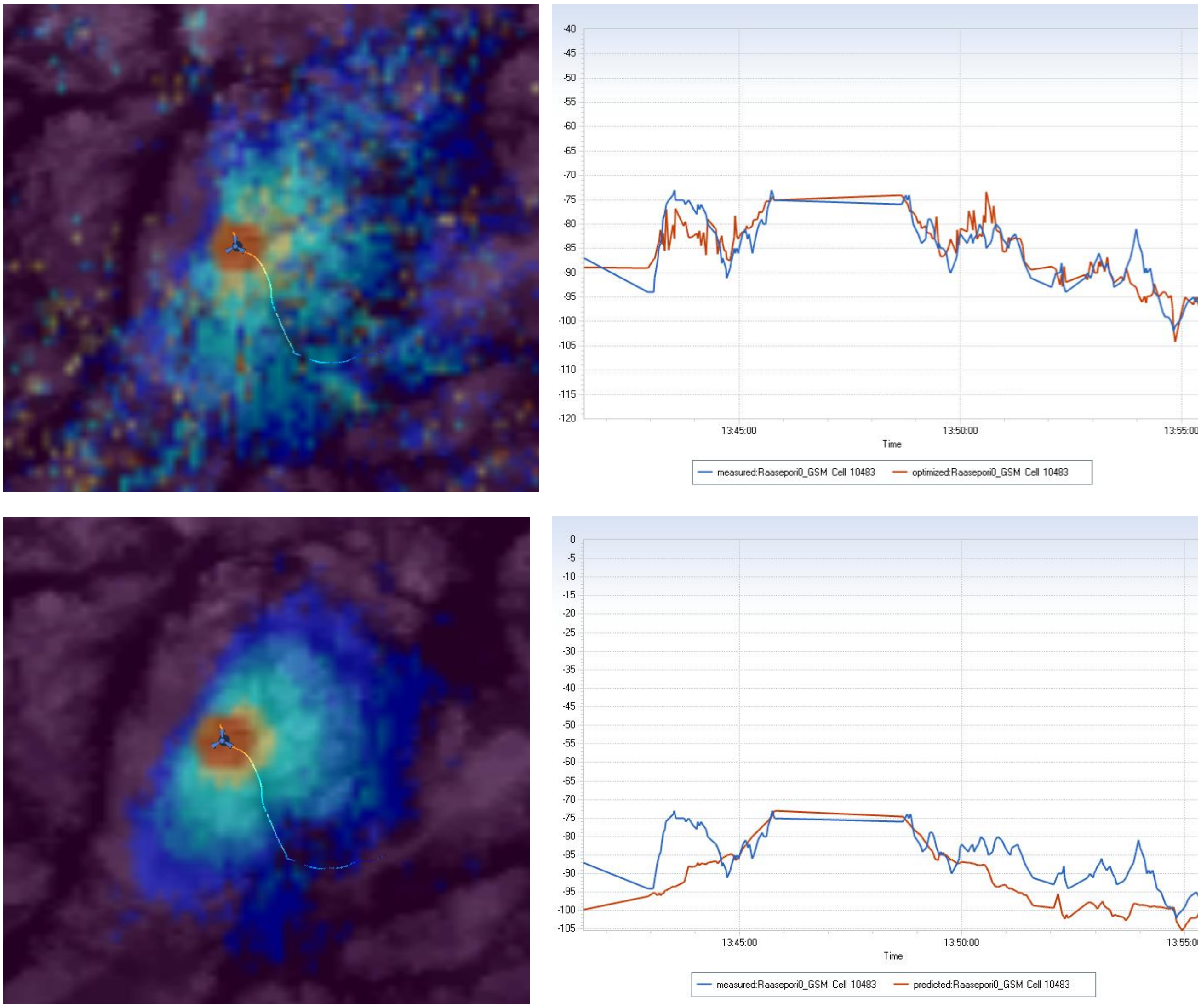

Figure 32. CCIRHata (long range) propagation model tuning using measurements from one cell.

The mast locations of UMTS900 or GSM900 networks were not available. Therefore, one task was to find a realistic estimate for cell sizes in GSM900 and UMTS900 networks in rural and suburban areas using propagation model calculations and field measurements. Based on the DL measurements, the cell size was found to be around 6 km. However, the transmission power in the UL direction (presented in Table 2) is significantly lower, and thus the cell size was reduced. For the simulations, the average radius of GSM900 cell was estimated to be 3 km in rural areas, and 1 km in suburban areas. These values will be validated during the FP3 when more GSM900 measurements are available.

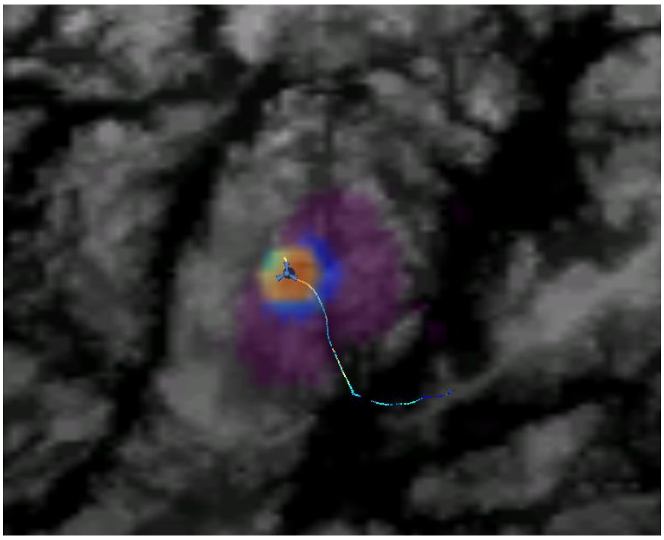

Figure 33. CCIRHata (long range) propagation model results in the UL direction.

4.5.2 Coverage rasters

The GSM900 network model was generated with the help of MML's mast data, input from SGEM partners, and preliminary link budget calculations. In addition, RF parameters were refined using Nemo Handy measurements and literature surveys. Figure 34 presents the computed coverage raster for GMS900 network in Raasepori region. Coverage rasters of GSM900 cells are overlapping. The network level coverage raster is created by taking the strongest value from the cell rasters. From the figure, we can see that there is close to 100 % coverage in Raasepori area.

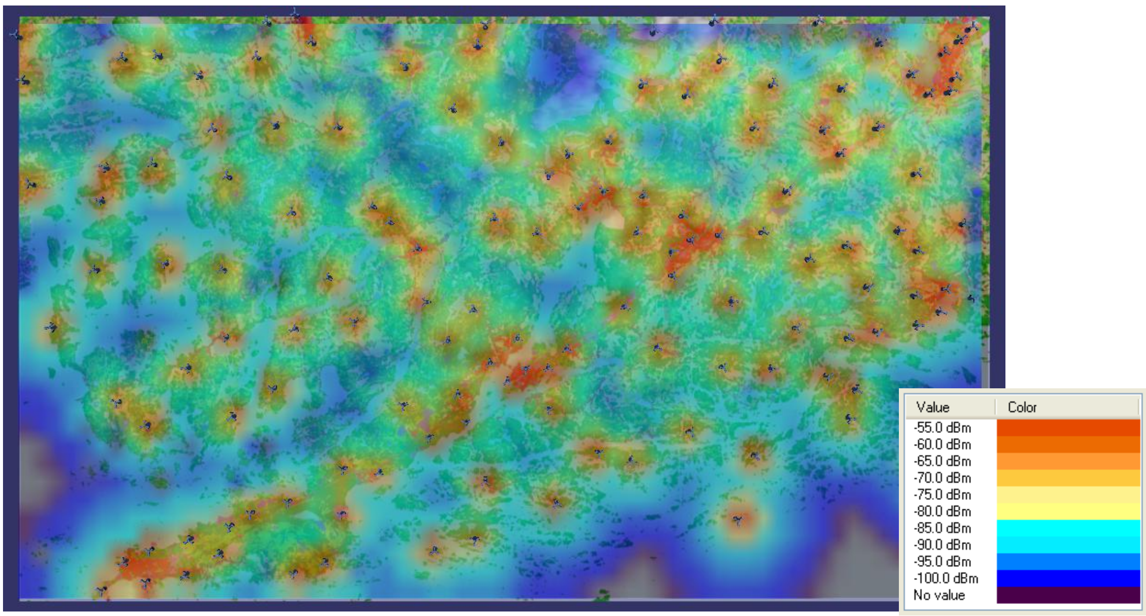

Figure 34. GSM900 coverage in Raasepori region.

The second picture shows an example of UMTS900 network that was generated according to Figure 6. It is evident that the picture does not contain all the sites, only the planned ones.

TeliaSonera's coverage map for UMTS900 can be found from [15]. To create a more precise model of UMTS900 network, additional field measurements will be carried out in spring 2012. The figure is just illustration that it is possible to create the network also for UMTS900 if all the required information would be available.

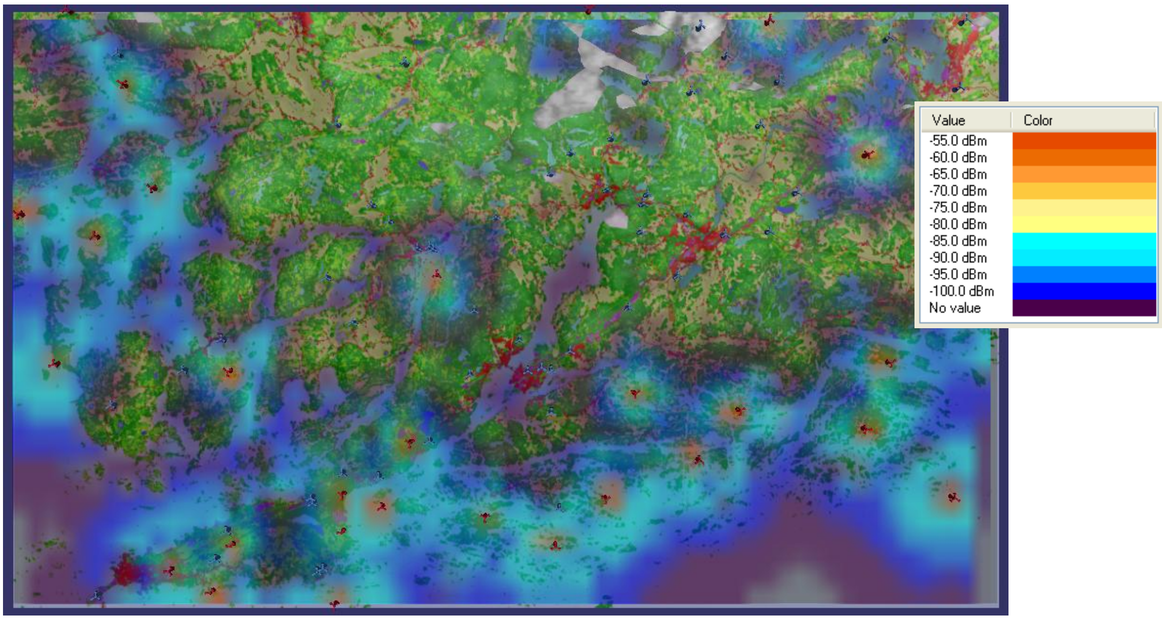

Figure 35. UMTS900 coverage in Raasepori region based on [6].

4.5.3 Redundancy

The redundancy raster is created by computing how many cells are exceeding the given threshold value at each raster location. The threshold value will be set according to the receiver's capabilities and used services (e.g. the received signal strength affects the used modulation). In the simulation model, each basestation site has typically three antenna sectors so the number of cells is approximately three times the number of masts. The next figure shows an example of computed redundancy raster for Raasepori region. Only cells that are energized are included to the computation. The picture below shows that the redundancy is high in suburban areas and along the roads (red colors in figure below). This indicates that the measured cell counts may be a bit too optimistic if we think about the whole Raasepori region. Therefore, additional measurements further away from main roads are needed to validate the redundancy analysis results.

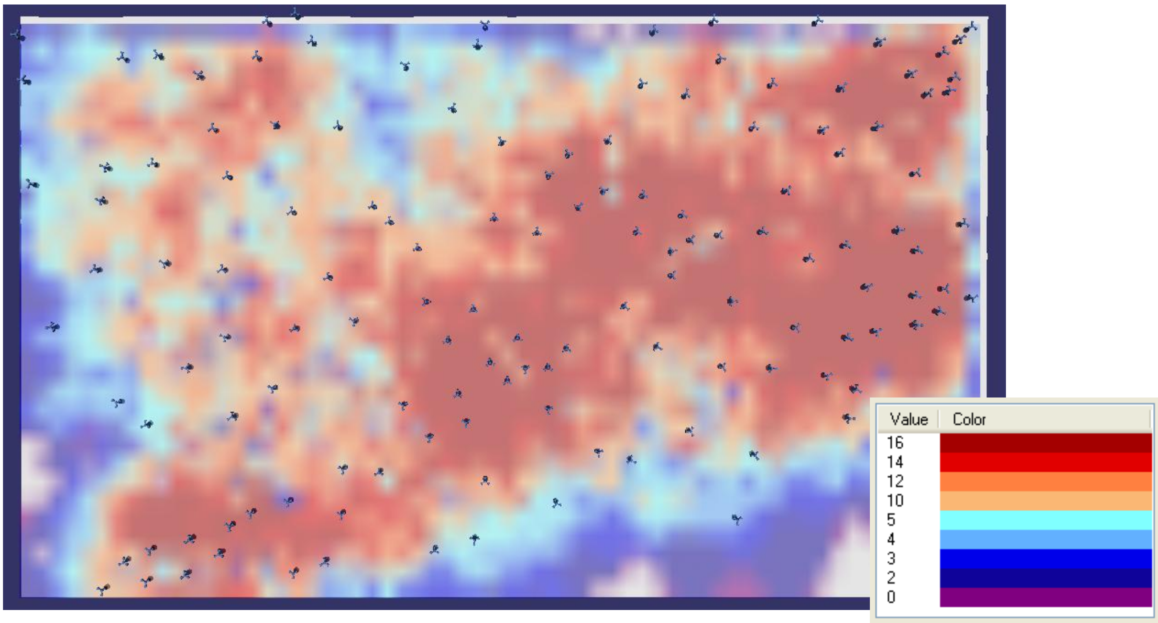

Figure 36. Number of hearable cells in GSM900 network.

4.5.4 Preliminary fault analysis

The fault analysis is done by creating failures in primary substation and feeder level to the modeled electric distribution network. The fault cases were the following ones:

- Case A: A feeder breaks down
- Case B: A primary substation breaks down
- Case C: 30 % of primary substations break down due to heavy storm

The effects of failure cases are compared to the normal situation where all GSM900 masts are energized. The green color in Figure 37 indicates that the mast is energized. The coverage and cell count rasters in a normal situation are presented in Figure 34 and Figure 36 respectively. The analysis is done in the DL direction and the receiver sensitivity level was set to -102 dBm.

Table 4. Fault statistics (normal situation)

Name	Description
Avg. Cell count (DL)	11.5
Redundancy probability (DL)	97.3 %
Element	Switched off (%)
Primary substations	0.0 %
Feeders	0.0 %
Secondary substations	0.0 %
Masts	0.0 %

Figure 37. Normal situation where all GSM900 masts are energized.

The percentage of geography area covered with at least *n* cells in normal situation is presented in Table 5. The maximum number of reported neighbor cells by a GSM terminal is seven. At least 75 % of geography area exceeds this threshold limit.

Table 5. Number of 'hearable' GSM900 cells in the DL direction.

Number of heard cells	Coverage Percentage
> 0	97.3 %
> 1	96.4 %
> 3	89.9 %
> 7	75.1 %
> 11	49.1 %

Case A: One feeder is down

In this failure case, one feeder has broken down. Consequently, a small number of secondary substations (shown in red) and GSM900 masts get de-energized. The average cell count drops slightly and the lost of one feeder causes a small hole to the GSM900 coverage, because also the closest neighboring cells are cut off from the power supply. The redundancy probability drops only slightly.

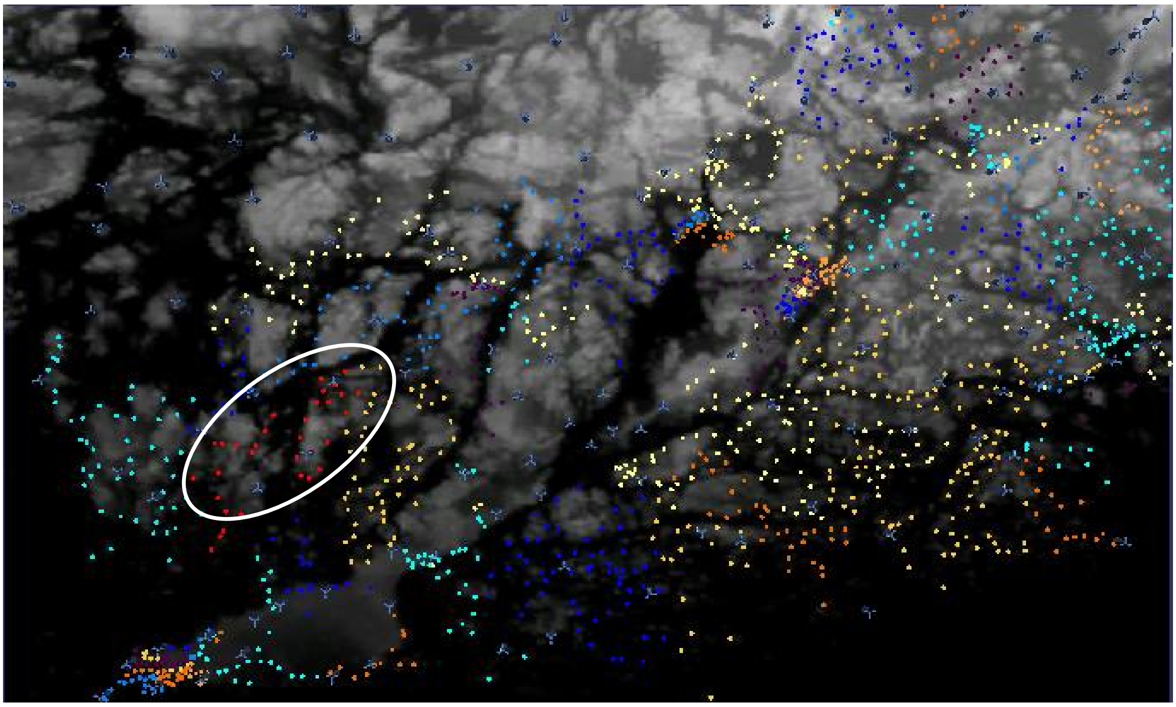

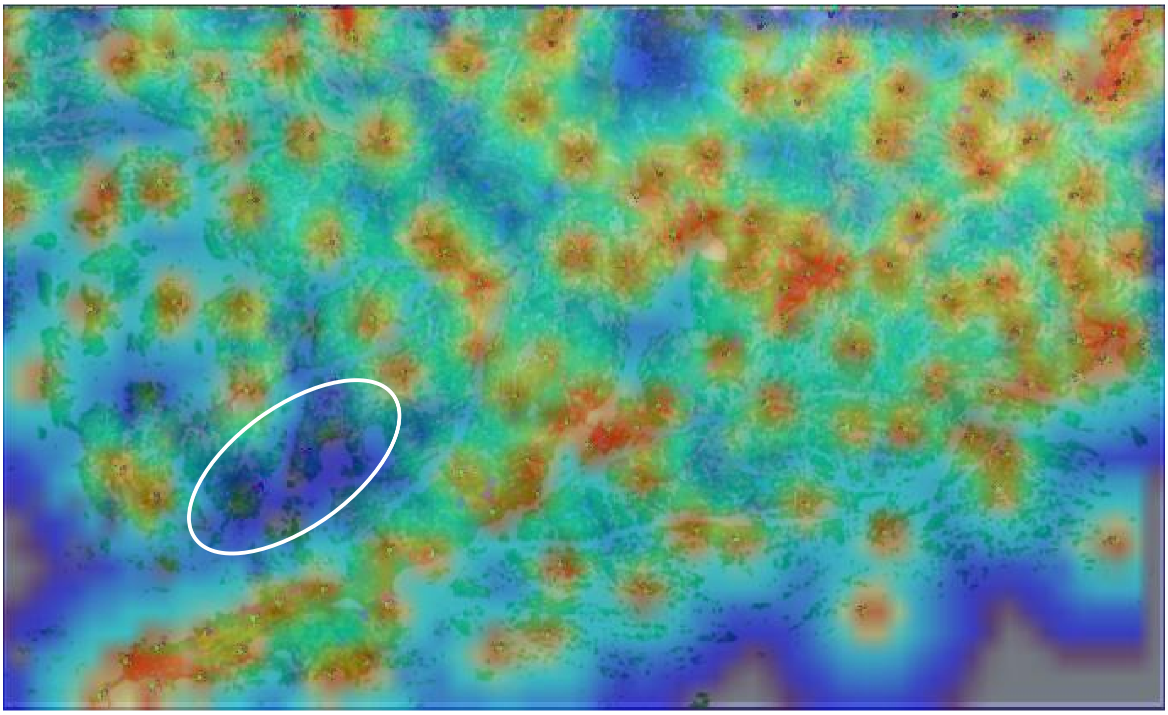

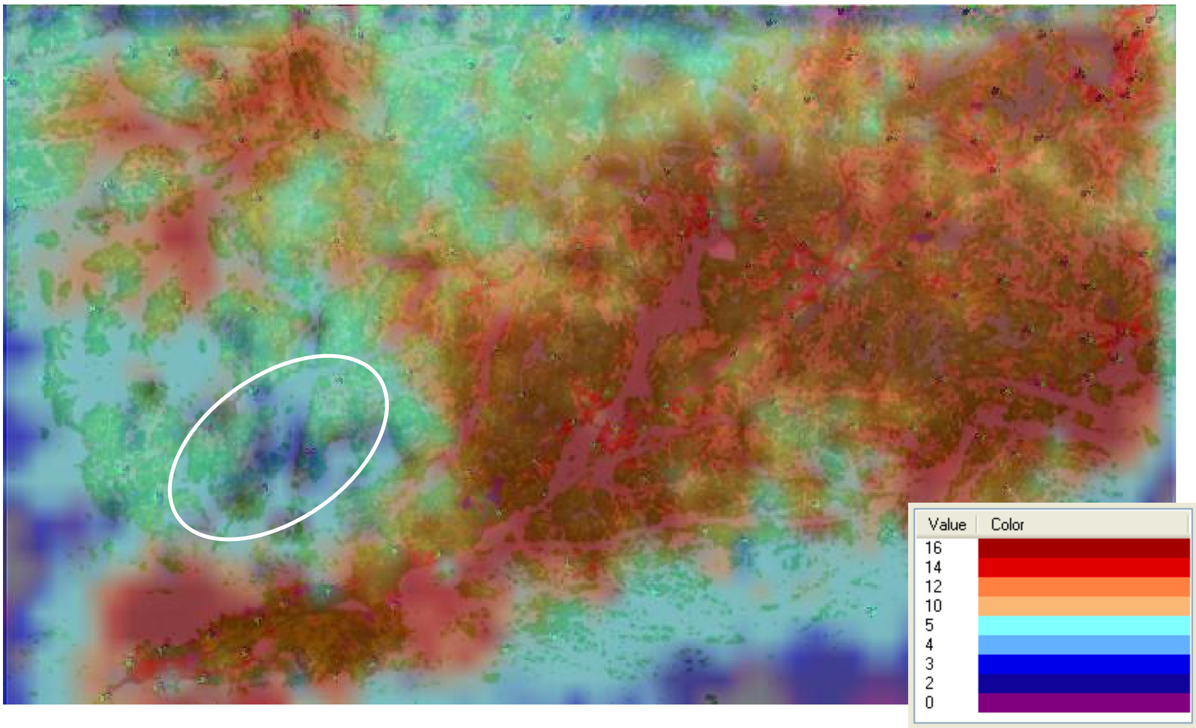

Figure 37. Result rasters when one feeder has broken down.

Table 6 Fault statistics (one feeder breaks down)

Name	Description
Avg. Cell count (DL)	11.1
Redundancy probability (DL)	97.2 %
Element	**Switched off (%)**
Primary substations	0.0 %
Feeders	1.1 %
Secondary substations	2.3 %
Masts	2.9 %

CASE B: One primary substation is down

In this failure case, one primary substation has broken down. The fault area grows, because the fault affects several adjacent feeders. Consequently, more neighboring GSM900 masts get de-energized. The average cell count drops from 11.1 to 10.5. The hole in coverage raster grows as more neighboring masts get cut off from the power supply

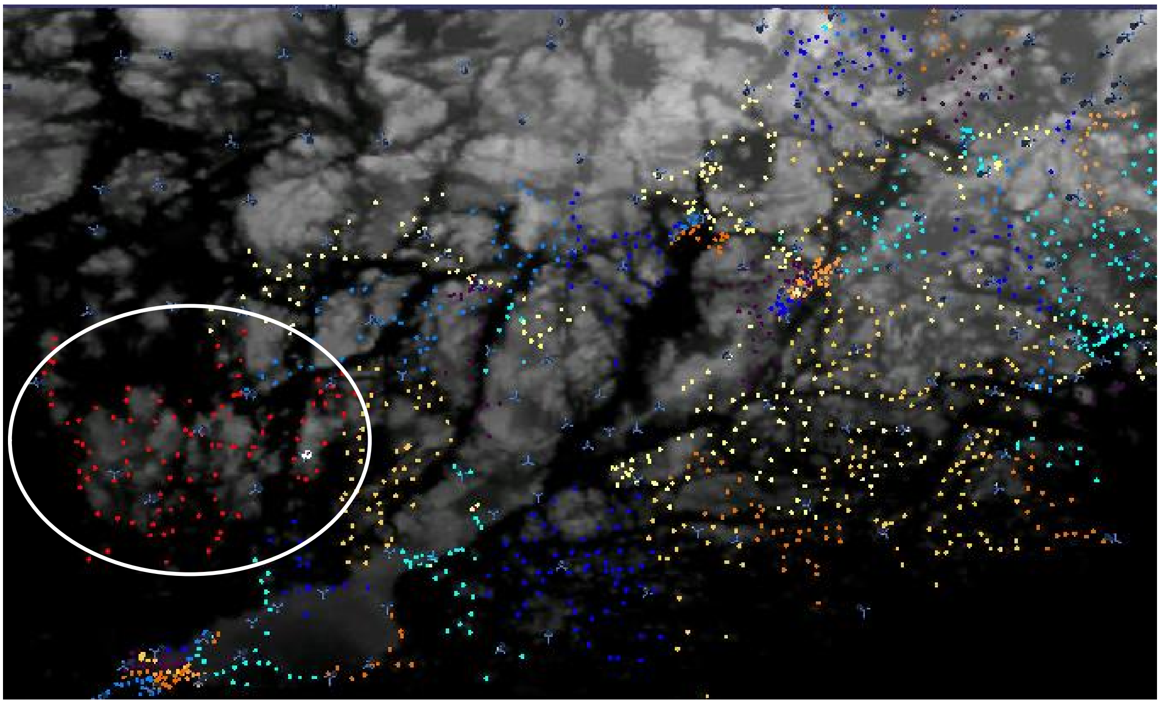

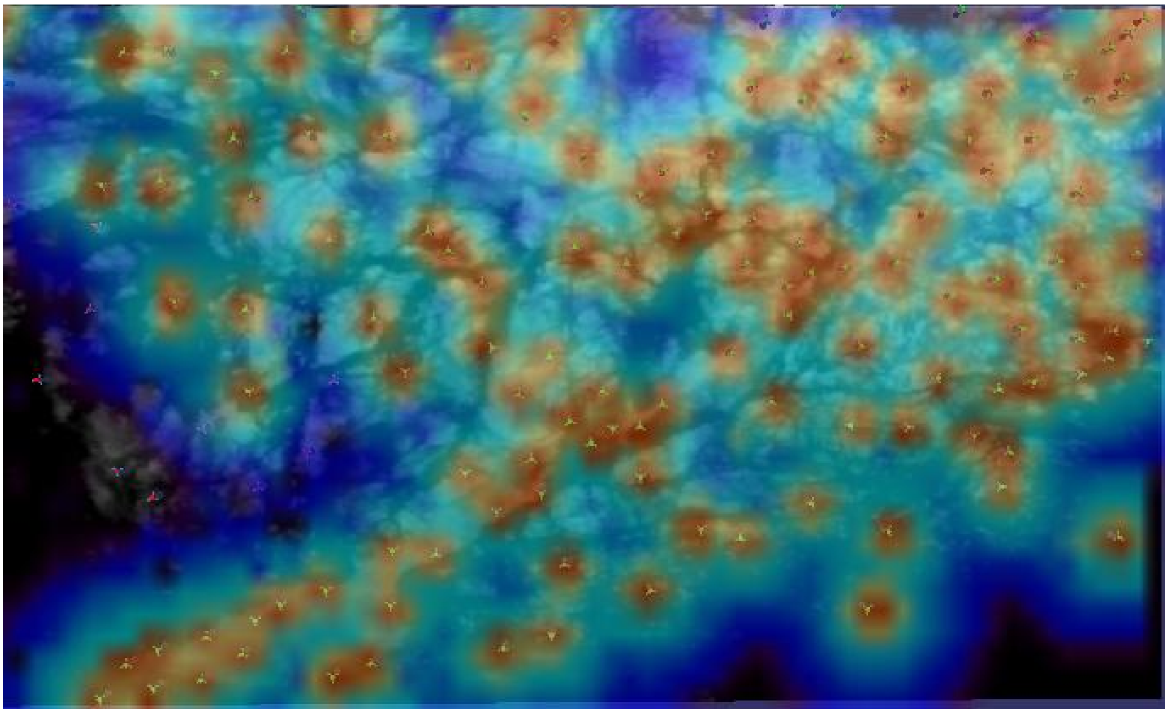

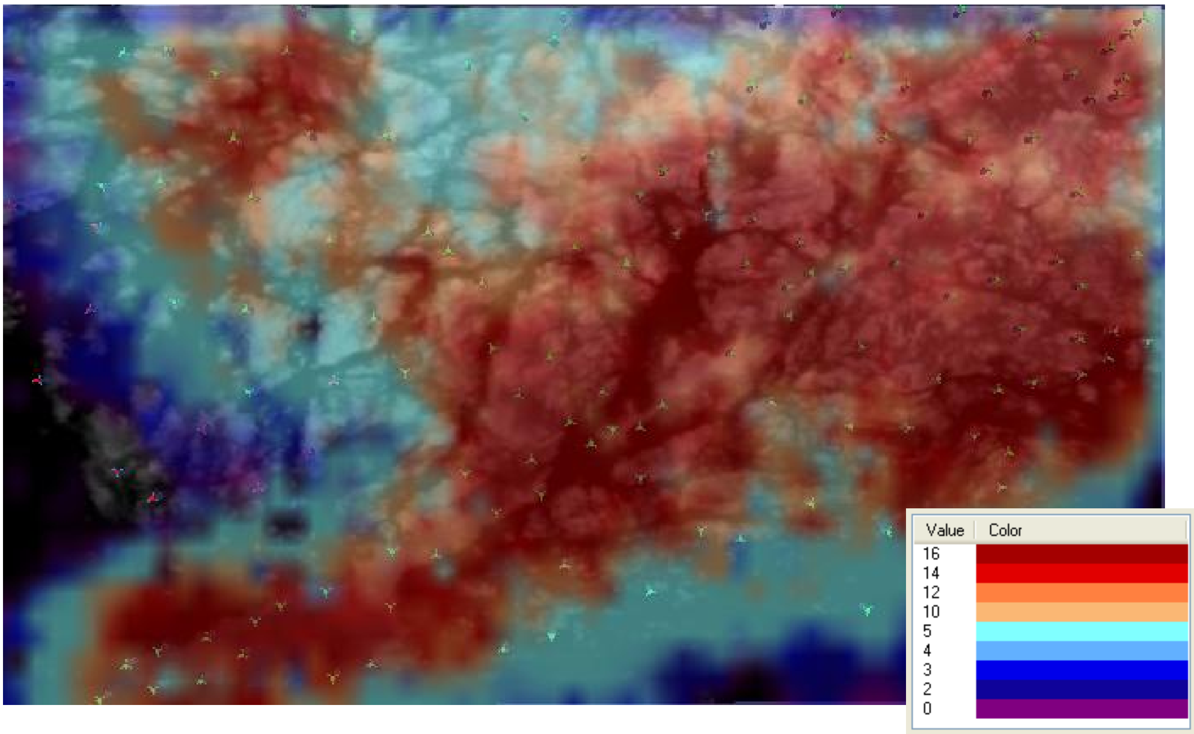

Figure 37. Result rasters when one primary substation has broken down.

Table 7. Fault statistics (one primary substation breaks down).

Name	Description
Avg. Cell count (DL)	10.5
Redundancy probability (DL)	93.6 %
Element	**Switched off (%)**
Primary substations	4.8 %
Feeders	4.7 %
Secondary substations	6.8 %
Masts	8.7 %

CASE C: 30 % of primary substations are down

The last failure case illustrates a heavy storm that breaks down approximately 30 % of the primary substations. Two distinctive fault regions appear. The average cell count drops from 10.5 to 7.47. Over 40 % of secondary substations are cut off but the redundancy probability drops only 3 %. The holes in the coverage raster in coastline area are more severe, because there are less surrounding feeders and masts to reduce the coverage hole. The inland areas are thus better secured against heavy storms.

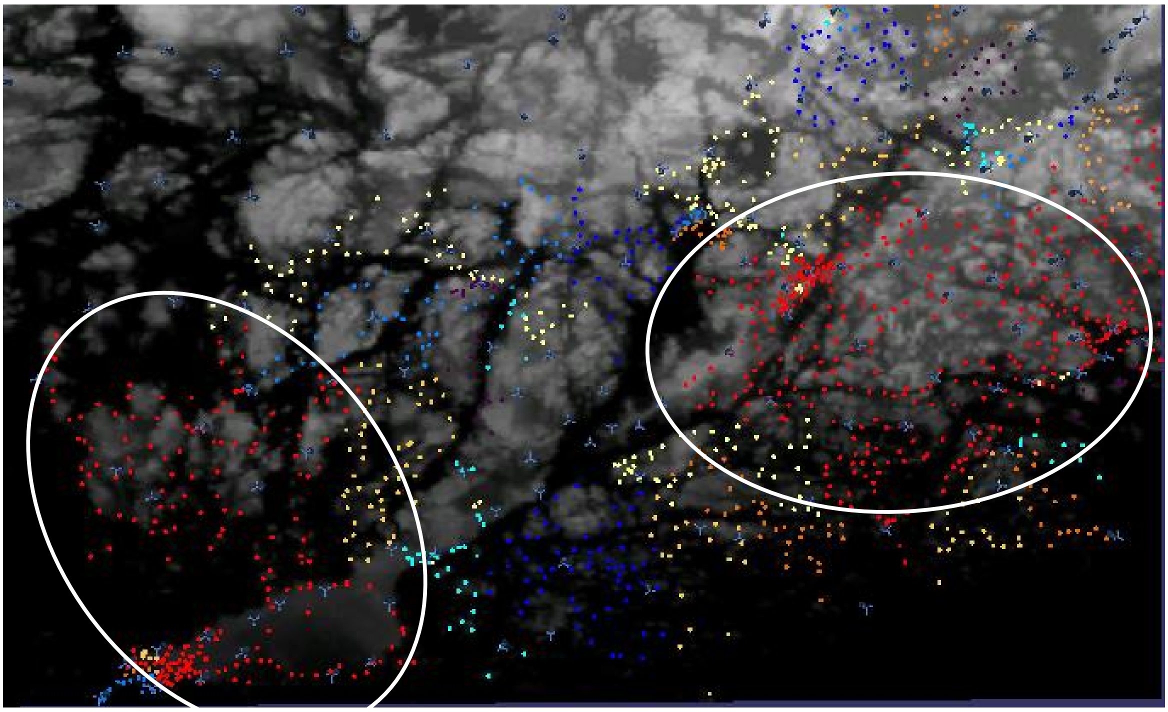

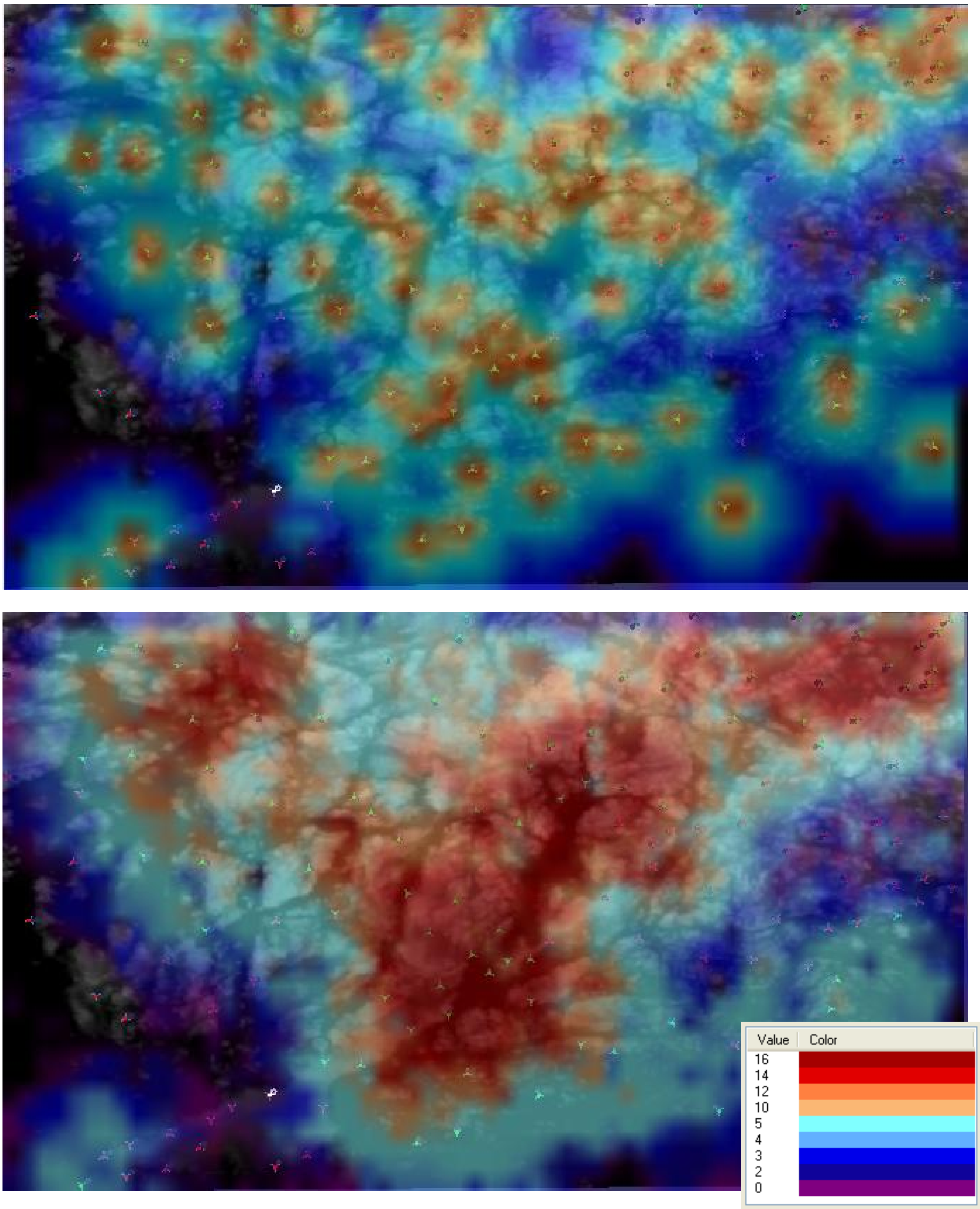

Figure 37. Result rasters when 30% of primary substations have broken down.

Table 8. Fault statistics (30% of primary substations have broken down).

Name	Description
Avg. Cell count (DL)	7.47
Redundancy probability (DL)	91.0 %
Element	**Switched off (%)**
Primary substations	35.0 %
Feeders	41.9 %
Secondary substations	43.4 %
Masts	38.7 %

5 Conclusions

This report sums up the work done so far to analyze the feasibility of commercial UMTS900/GSM900 networks for the Smart Grid communication in rural and suburban areas. The preliminary field measurements and calculation results are a good basis for realistic simulations. It is evident that additional field measurements are needed e.g. for calibrating propagation models, refining RF parameters, fine-tuning correction terms for different clutter types, and adjusting base stations' locations. At this stage, simulation results already indicate that there is a lot of inherent redundancy in public wireless networks. The study shows that approximately 11.5 base stations can be heard in the DL direction in Raasepori area. Obviously, in the UL direction, the cell count is anticipated to be a little smaller. Our simulations show, that less than 3% of the area is such, that no base station can be heard; mostly in sea areas. Furthermore, we found out that at least two cells can be heard in 96.4 % of the Raasepori area. According to the simulations, the faults in feeder level can easily be compensated by neighbouring cells powered by other feeders. Thus, a single feeder fault is not likely to cause notable problems to the smart grid communication. If the breakdown of a complete primary substation happens, then the fault area grows and neighbouring cells are also affected. As a result, adjacent cells are not able to fully compensate the lost coverage. To eliminate the coverage hole, it would require planned use of reclosers and disconnectors. In case of a heavy storm, coastal areas are found to be more vulnerable, because they are not so well surrounded by other feeders as inland areas.

The next step is to enhance the simulation tool to include disconnectors and reclosers to the simulation model and to perform defined failure scenarios in UMTS900 network. In spring 2012, results from preliminary simulations and measurements will be analyzed jointly with the results presented in NSN's technical report [16], which studies advanced Smart Grid communication concepts on national level. The aim is to utilize its observations to make our simulations more precise, and vice versa to offer input to the national level model or even prove its validity in the Raasepori case.

The next phase (FP3) will concentrate on

- Finalizing the electric distribution network model

- Constructing UMTS network configuration and setting its RF parameters
- Developing a method to collect automatically UMTS900 measurement samples during the drive measurement.
- Planning and performing the additional field measurements to calibrate propagation and clutter models and to refine RF parameters of the communication networks
- Considering base station’s battery back-up aspects
- Performing simulations with defined failure scenarios
- Writing a final report about the results and providing input to other WP6 tasks.

The following topics have also been discussed but they require significant efforts and contributions from other SGEM II partners:

- Including urban areas to the simulations (building data is needed)
- Making preliminary calculations with a LTE network and using field measurement results obtained from other tasks (propagation models need to be enhanced to include LTE aspects)
- Finding strategies to include additional protection and control zones to electric distribution networks in order to improve the SAIDI and SAIFI (involvement of energy companies)
- Making an interface to exchange information between an electric distribution maintenance system and the simulation tool (involvement of energy companies).

6 Background information on BS battery backup requirements

In Finland BS battery backup requirements are set by the Finnish Communications Regulatory Authority (Ficora) and can be found in [15,16]. The key requirements from [16] are extracted as follows:

Taulukko 1: Tärkeysluokat

Tärkeysluokka	Viestintäverkon tai -palvelun komponentti
1	Komponentti, joka vaikuttaa viestintäpalveluihin erittäin suurella maantieteellisellä alueella tai komponentti, joka vaikuttaa suuruusluokaltaan • ≥ 200 000 käyttäjän puhelinpalveluun tai • ≥ 200 000 käyttäjän laajakaistapalveluun tai • ≥ 500 000 käyttäjän sähköpostipalveluun tai • ≥ 300 000 käyttäjän joukkoviestintäpalveluun tai • ≥ 500 000 käyttäjän muuhun viestintäpalveluun.
2	Komponentti, joka vaikuttaa viestintäpalveluihin suurella maantieteellisellä alueella tai komponentti, joka vaikuttaa suuruusluokaltaan • ≥ 50 000 käyttäjän puhelinpalveluun tai • ≥ 50 000 käyttäjän laajakaistapalveluun tai • ≥ 200 000 käyttäjän sähköpostipalveluun tai • ≥ 100 000 käyttäjän joukkoviestintäpalveluun tai • ≥ 200 000 käyttäjän muuhun viestintäpalveluun.
3	Komponentti, jota vaikuttaa • ≥ 150 GSM-verkon puhekanavan toimintaan tai • ≥ 1000 käyttäjän puhelinpalveluun tai • ≥ 1200 käyttäjän laajakaistapalveluun tai • ≥ 50 000 käyttäjän sähköpostipalveluun tai • ≥ 50 000 käyttäjän joukkoviestintäpalveluun tai • ≥ 100 000 käyttäjän muuhun viestintäpalveluun.
4	Joukkoviestintäverkon päälähetin tai komponentti, joka vaikuttaa • ≥ 75 GSM-verkon puhekanavan toimintaan tai • ≥ 250 käyttäjän puhelinpalveluun tai • ≥ 250 käyttäjän laajakaistapalveluun tai • ≥ 10 000 käyttäjän sähköpostipalveluun tai • ≥ 50 000 käyttäjän muuhun viestintäpalveluun.
5	• Matkaviestinverkon peruspeiton tukiasema tai • kiinteän puhelinverkon keskitin tai • laajakaistakeskitin tai • kiinteän langattoman laajakaistaverkon tukiasema tai • maanpäällisen televisioverkon täytelähetin, joka palvelee yli 50 kotitaloutta tai • radiotoiminnan täytelähetin tai • komponentti, joka vaikuttaa yleisessä puhelinverkossa toimiviin puhelinpalveluihin tai • komponentti, joka vaikuttaa yli 1 000 käyttäjän sähköpostipalveluun.

Taulukko 2: Tehonsyötön varmistaminen

Tärkeysluokka[7)]	Akuston [1)] varmistusaika	Varavoimalaitos ja muut vaatimukset
1	≥ 3 tuntia	Kiinteä varavoimalaitos, jonka varmistuksena on: [2)] - kiinteän varavoimalaitoksen N+1 -varmistus tai - vähintään 6 tunnin akustovarmistus tai - käytettävissä oleva siirrettävä varavoimalaitos liitäntämahdollisuuksineen
2	≥ 6 tuntia [3)]	Kiinteä varavoimalaitos tai käytettävissä oleva siirrettävä varavoimalaitos liitäntämahdollisuuksineen
3	≥ 12 tuntia [3), 4)]	Siirrettävän varavoimalaitoksen liitäntämahdollisuus, mikäli varavoimalaitoksen käyttö on kohteessa mahdollista
4	≥ 6 tuntia [3), 5)]	Siirrettävän varavoimalaitoksen liitäntämahdollisuus, mikäli varavoimalaitoksen käyttö on kohteessa mahdollista
5	≥ 3 tuntia [6)]	Siirrettävän varavoimalaitoksen liitäntämahdollisuus, mikäli varavoimalaitoksen käyttö on kohteessa mahdollista

1) Maanpäällisen joukkoviestintäverkon lähettimille ei vaadita akustoa, mikäli lähettimen tehonsyöttö on varmistettu kiinteällä varavoimalaitoksella.
2) Kiinteän varavoimalaitoksen varmistusta ei vaadita maanpäällisen joukkoviestintäverkon lähettimiltä, mikäli varmistusta ei ole toteutettavissa kohtuullisin kustannuksin.
3) Jos viestintäverkon tai -palvelun komponentti on kytketty voimalaitejärjestelmään, jossa tehonsyötön varmistuksena on kiinteä varavoimalaitos, akuston minimivarmistusajaksi riittää 3 tuntia.
4) Jos viestintäverkon tai -palvelun komponentti sijaitsee taajamassa, akuston minimivarmistusajaksi riittää 6 tuntia.
5) Mikäli vähintään kolme taajaman ulkopuolella sijaitsevaa tärkeysluokan 4 viestintäverkon tai -palvelun komponenttia käyttää yhteistä yleisen sähköverkon liitäntää, ja komponenttien tehonsyötön varmistuksena ei ole kiinteää varavoimalaitosta, tulee akuston minimivarmistusaika pidentää 12 tuntiin.
6) Mikäli laitetilaan ei ole mahdollista päästä akuston 3 tunnin minimivarmistusajan puitteissa laitetilan kaukaisen sijainnin, maasto-olosuhteiden tai odotettavissa olevien keliolosuhteiden vuoksi, tulee akuston minimivarmistusaika pidentää 6 tuntiin.
7) Tärkeysluokalla tarkoitetaan 3 §:ssä määriteltyä viestintäverkon tai -palvelun komponentin tärkeysluokkaa.

As long as GSM provides the ‘baseline coverage’, i.e. prior to replacement by UMTS900, GSM BS are in the ‘importance class 5’ and should provide ≥ 3 h battery backup, with a possibility to connect backup generators, but see footnote 6).

UMTS BS has a requirement of 15 min battery backup [15].

The philosophy is to set stringent requirements for the radio system components providing baseline radio coverage which is, today, GSM. More lenient requirements are set for system components providing additional capacity (e.g. UMTS cells overlaid on a GSM system, GSM microcells, etc.).

However, it is mentioned in [16] that should UMTS become the radio to provide baseline coverage (this could happen e.g. when GSM900 migrates to UMTS900) then the above more stringent requirements will need to be considered for UMTS BS and RNC and updates of this regulation are expected. This means that M2M devices (RTUs) with multi-band/mode functionality can expect to find a fall-back to a battery protected baseline 3GPP system.

The 3… 6 h BS battery backup times mandated by Ficora appear to be quite well matched to get across most power faults: a glance at the 2009 statistics of fault interruption times, Fig. 5.3 from [19] suggests that a large proportion of isolated faults in rural areas can be cleared already within 4 h. A large gain from FA, i.e. to be able to operate remote controlled RTUs, is already obtained by having at least 1 h BS battery backup time:

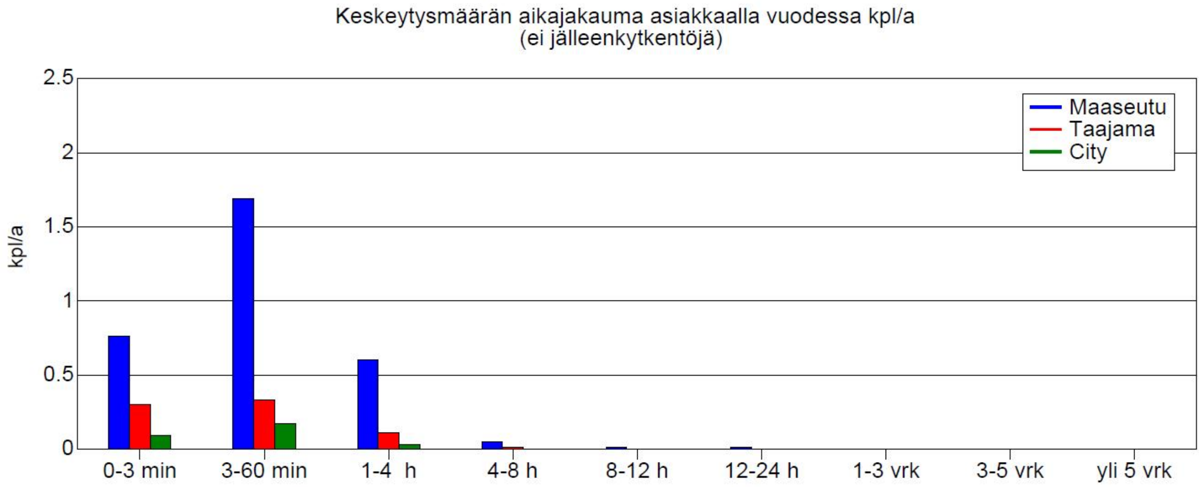

Finland 2009 distribution of customer interruption times per year, from [19]

Rural MV FA investment makes economic sense when the time, without automation, for fault detection & isolation + feeder reconfiguration is of the same order as times for fault clearance. In case of major storms and related very large scale power outages, however, the potential benefit of remote controlled FA, when compared to more isolated faults, will be diminished due to:

- in case of a large amount of faults there is much less scope for remote controlled FA to be effective for fault isolation and switching of alternative power connections (such as closing of N.O. disconnectors)
- a larger amount of utility service crews will have to be in the affected area anyway
- in this case customer interruption times are dominated by fault repair times
- also the battery back-up of the IEDs is limited to some 48 h, hence outage/repair times in the order of days cannot be bridged.

While there might still be some benefit for remote controlled FA in case of storms in terms of reducing FDIR times for some customers, it appears that it is not reasonable and economically justified from a M2M perspective, to design the public communication system availability and power backup requirements for wide scale and long lasting (several days) power outages.

The main interest of this study in inherent reliability are therefore power outages which are longer than typical BS battery back times (≥ 3 h), but on the other hand neither of very large scale nature nor significantly longer than the IED battery backup times (<48h).

7 Abbreviations

2G	Second Generation
3D	Three Dimensional
3G	Third Generation
3GPP	Third Generation Partnership Program
4G	Fourth Generation
ARFCN	Absolute Radio Frequency Channel Number
BSIC	Base Station Identity Code
BTS	Base station
CLC	Corine Land Cover
CLC2006	Corine Land Cover classes 2006
CORINE	Coordinate Information on the Environment
DA	Device Application
dB	Decibel
dBi	Decibel Isotropic
dBm	Power ratio in decibels (dB) of the measured power referenced to one milliwatt
DL	Downlink
DMS	Distribution Management System
DR	Delayed Reclosure
DSO	Distribution System Operator
EDGE	Enhanced Data rates for GSM Evolution
EIRP	Effective Isotropic Radiated Power
ESB	Electricity Supply Board
FA	Feeder Automation
FICORA	Finnish Communications Regulatory Authority
FP3	Funding Period 3
GIS	Geographic Information System
GMES	Global Monitoring for Environment and Security

GPRS	General Packet Radio Service
GPS	Global Positioning System
GSM	Global System for Mobile Communications
GSM900	Global System for Mobile Communications at 900 MHz
GSMA	GSM (Groupe Spéciale Mobile) Association
HCS	Hierarchical Cell Structures
HSR	High Speed Reclosure
IP	Internet Protocol
LAC	Location Area Code
LSA	Link State Algorithms
LTE	Long Term Evolution
M2M	Machine-to-Machine
MML	Maanmittauslaitos
MS	Mobile Station
MV	Medium Voltage
N.O.	Normally open
RAC	Routing Area Code
RF	Radio Frequency
RMU	Ring Main Unit
RNC	Radio Network Controller
RSSI	Received signal strength indication
RTU	Remote Terminal Unit
RX	Receiver
SAIDI	System Average Interruption Duration Index
SAIFI	System Average Interruption Frequency Index
SCADA	Supervisory Control And Data Acquisition
SGEM	Smart Grids and Energy Markets
SNR	Signal-to-Noise Ratio
SYKE	Suomen ympäristökeskus
TDMA	Time Division Multiple Access
TX	Transmitter
UL	Uplink
UMTS	Universal Mobile Telecommunications System
UMTS900	Universal Mobile Telecommunications System at 900 MHz
XML	Extensible Markup Language

8 References

[1] J. Penttonen, Effect of Expanding Cell Radius and it's Impact on Cellular Smart Grid Applications, Discussion paper, year 2011.

[2] http://violasystemscom.adv3.nebula.fi/sites/default/files/Vattenfall%20case.pdf

[3] http://violasystemscom.adv3.nebula.fi/sites/default/files/ESB%20case.pdf

[4] J. Penttonen, Inherent Redundancy in Public Wireless, Networks, Applications in Smart Grid, white paper, year 2011.

[5] Finnish Environment Institute, CLC2006 Finland, Final technical report, November 2009.

[6] TeliaSonera's planned UMTS900 sites, http://www.sonera.fi/asiakastuki/puhelin+ja+liittymat/kuuluvuus+ja+nopeuskartta/rakenteila+olevat+verkot

[7] Kema Inc, Why Mobile for Smart Utilities? Assessing Service Opportunities in the Utility Sector for the Mobile Network Industry, Report for the GSMA, June 2011.

[8] Viola Systems: Case Vattenfall: Automating the Distribution Network, http://www.automation.com/pdf_articles/Vattenfall_Viola.pdf

[9] http://en.wikipedia.org/wiki/Electrical_substation (link checked 11.12.2011)

[10] http://en.wikipedia.org/wiki/Recloser (link checked 11.12.2011)

[11] http://en.wikipedia.org/wiki/Disconnector (link checked 11.12.2011)

[12] http://en.wikipedia.org/wiki/Composite_pattern (link checked 11.12.2011)

[13] L. Helenius, SGEM II Raasepori 2G/3G field measurements, 2011.

[14] Anite, Nemo File Format Specification, ver 2.05, Last updated April 2010.

[15] http://www.sonera.fi/asiakastuki+ja+edut/puhelin+ja+liittymat/kuuluvuus+ja+nopeuskartta/kuuluvuuskartta

[16] P. Muszynski, D6.1.3 Advanced Smart Grid Communication Concept, NSN, 2011.

[17] D4.1.4.3: Optimal Concepts for Smart Grid Communication, SGEM FP1, H. Elias & P. Muszynski, http://research.cleen.fi/research/images/e/e2/RTENOTITLESGEM_D4143_v2.pdf

[18] Ficora: Viestintävirasto 54/2008 M, VIESTINTÄVERKKOJEN JA -PALVELUJEN VARMISTAMISESTA, helmikuuta 2008 http://www.ficora.fi/attachments/suomiry/5vB4GW4xt/Viestintavirasto542008M.pdf

[19] Ficora: MÄÄRÄYKSEN 54 PERUSTELUT JA SOVELTAMINEN VIESTINTÄVERKKOJEN JA PALVELUIDEN VARMISTAMISESTA, 14.2.2008 http://www.ficora.fi/attachments/5kAoklazG/MPS54.pdf

[20] Lakervi, Holmes: Electricity Distribution Network Design, The Institution of Engineering and Technology

[21] Lakervi, Partanen: Sähkönjakelutekniikka, OTATIETO / YLIOPISTOKUSTANNUS 2008

[22] Energiateollisuus: KESKEYTYSTILASTO 2009, http://www.energia.fi/fi/tilastot/keskeytystilastot/keskeytystilasto%202009.html

[23] Energiateollisuus: KESKEYTYSTILASTO 2010, http://www.energiamarkkinavirasto.fi/files/Kes%C3%A4n%202010%20myrsky%20raportti_lopullinen%20_2_.pdf